

The Higgs boson - its implications and prospects for future discoveries

Steven D. Bass^{1,2}, Albert De Roeck^{3,4}, and Marumi Kado^{5,6}

¹Kitzbühel Centre for Physics, Kitzbühel, Austria.

²Jagiellonian University, Marian Smoluchowski Institute of Physics, Kraków, Poland.

³CERN, Experimental Physics Department, Geneva, Switzerland.

⁴University of Antwerp, Physics Department, Antwerp, Belgium.

⁵INFN Sezione di Roma and Dipartimento di Fisica, Sapienza Università di Roma, Rome, Italy.

⁶IJCLab, Université Paris-Saclay, CNRS/IN2P3, 91405, Orsay, France.

ABSTRACT

The Higgs boson, a fundamental scalar, was discovered at CERN in 2012 with mass 125 GeV, a mass that turned out to be a remarkable choice of Nature. In the Standard Model of particle physics, the Higgs boson is closely linked to the mechanism that gives mass to the W and Z gauge bosons that mediate the weak interactions and to the charged fermions. Following discovery of the Higgs boson, present measurements at the Large Hadron Collider are focused on testing the Higgs boson's couplings to other elementary particles, precision measurements of the Higgs boson's properties and initial investigation of the Higgs boson's self-interaction and shape of the Higgs potential. With the Higgs boson mass of 125 GeV the vacuum sits very close to the border of stable and metastable, which may be a hint to deeper physics beyond the Standard Model. The Higgs potential also plays an important role in ideas about the cosmological constant or dark energy that drives the accelerating expansion of the Universe, the mysterious dark matter that comprises about 80% of the matter component in the Universe, as well as a possible phase transition in the early Universe that might be responsible for baryogenesis. Detailed study of the Higgs boson is at the centre of the recent European Strategy for Particle Physics update. Here we review the present status of this physics and discuss the new insights expected from present and future experiments.

Key points:

- The discovery of the Higgs boson, the first ever observed elementary scalar particle, at CERN's Large Hadron Collider (LHC) in 2012 was a major milestone in the development of particle physics.
 - Besides confirming the mechanism which gives masses to the W and Z bosons, thus making the electroweak interaction short range, direct tests of the couplings of the Higgs boson to fermions are major achievements of the LHC program. A recent highlight is direct observation of the Higgs boson coupling to muons.
 - The observed properties of the Higgs boson put the Standard Model vacuum intriguingly very close to the border of stable and metastable. Further connections to the outstanding questions of baryogenesis, dark matter, dark energy and inflation mean that the Higgs boson is central to our understanding of the physical Universe.
 - Precision measurements of the Higgs boson to further probe its interactions and possible deeper origin and structure are an essential part of the High-Luminosity LHC program and were recently identified by the European Strategy for Particle Physics to be the highest priority for the next high-energy collider facility.

1 Introduction

The discovery of the Higgs boson in 2012 at CERN's Large Hadron Collider, LHC, in Geneva Switzerland by the ATLAS¹ and CMS² experiments was a key milestone for particle physics, rewarded by the award of the 2013 Nobel Prize for Physics to François Englert³ and Peter Higgs⁴. The Higgs boson is central to our understanding of particle physics. It is the first (and so far only) discovered seemingly elementary particle with spin zero.

The Standard Model⁵⁻⁷ provides an excellent description of particle physics experimental results so far, from collider experiments at the LHC⁸, with centre of mass energy up to 13 TeV⁹, to low-energy precision measurements including those of the fine structure constant^{10,11} of Quantum Electrodynamics, QED, and the electron's electric dipole moment¹². The matter of everyday experience is built of elementary fermions: quarks and leptons. Particle interactions are determined by local gauge symmetries and mediated by the exchange of spin-one gauge bosons. These are the massless photon for QED which binds electrons to nuclei in atoms, gluons for Quantum Chromodynamics, QCD, which bind quarks inside the proton and the massive

W and Z bosons for the weak interactions that power the sun and nuclear reactors. Symmetry drives the particle interactions. Invariance under local changes in the phases of fermion fields guarantees the dynamics. An important ingredient is the origin of particle masses. Within the Standard Model the masses of the W and Z gauge bosons and charged fermions come from coupling of these particles to the scalar spin-zero Higgs field which comes with a non-vanishing vacuum expectation value, vev, and a Higgs condensate filling all space.

While the discovered boson behaves very much like the Standard Model Higgs with a mass of 125 GeV, in which case it completes the particle spectrum of the Standard Model, important open puzzles remain connecting particle physics to cosmology that require extra new physics. These are the dark energy that generates the accelerating expansion of the Universe¹³, the matter-antimatter asymmetry in the Universe¹⁴, primordial inflation¹⁵ as well as the mysterious extra dark matter which comprises about 80% of the matter component in the Universe¹⁶. Considerable theoretical work has gone into thinking about possible connections between these open issues and the properties of the Higgs boson. The Higgs boson's observed decays to vector bosons indicate the existence of a Higgs boson condensate. While its mass was expected to be commensurate with the electroweak scale to ensure unitarity of the scattering of longitudinally polarized vector bosons, such a relatively small mass, which is very much less than the Planck scale that defines the limit of particle physics before quantum gravity effects might apply, raised the fundamental question of the naturalness of the Standard Model.

The European Particle Physics Strategy recently identified precision studies of the Higgs boson as the main priority for the next high-energy collider with measurements first at the planned high luminosity upgrade of the LHC and, later, with a dedicated Higgs factory as a new facility. This program involves essential interaction between experiment and theory. How well does the discovered boson match the Standard Model Higgs and can we find hints for new physics beyond the Standard Model?

This article surveys Higgs boson physics with an outlook to future experiments. In Section 2 we discuss the role of the Higgs boson in the origin of mass. Section 3 reviews the discovery and early measurements of the Higgs boson's properties. Recent measurements of the Higgs coupling to fermions are discussed in Section 4. Section 5 summarises the status of measurement of the Higgs boson's properties and interactions in comparison to the predictions for the Higgs boson described by the Standard Model. In Section 6 we discuss the Higgs self-coupling. Section 7 focuses on searches for any extra Higgs states or possible new CP violation in the Higgs sector. In Sections 8 and 9 we describe open theoretical issues connected to the Higgs boson in particle physics and cosmology. What might the Higgs boson be telling us about (the need for) extra new physics beyond the Standard Model? Finally, in Section 10 we give an outlook to future measurements that might shed light on these questions and the role of the Higgs in understanding the deep structure of the Universe.

2 The Higgs boson and massive gauge bosons

The Higgs story starts from the interplay of mass and gauge invariance. If taken alone, mass terms for gauge bosons break the underlying gauge symmetry. For example, consider particles (fermions or scalar bosons) χ interacting with a gauge field A_μ with the system invariant under the local gauge transformations $\chi \rightarrow e^{i\alpha}\chi$ and $A_\mu \rightarrow A_\mu + \frac{1}{g}\partial_\mu\alpha$ where g is the coupling of A_μ to χ . Introducing a mass term $m^2 A_\mu A^\mu$ violates the gauge symmetry without extra ingredients.

This problem is resolved through the Brout-Englert-Higgs (BEH) mechanism¹⁷⁻²⁰ with related work in Refs^{21,22}. The gauge symmetry of the underlying theory can be hidden in the ground state. The symmetry parameter α freezes out to a particular value with all possible values being degenerate. This process, which is known as spontaneous symmetry breaking, generates massless Goldstone modes – one for each generator of the symmetry. For local gauge symmetries these massless Goldstone modes combine with the gauge bosons to generate new longitudinal modes of the gauge fields, conserving the total number of degrees of freedom. The transverse and longitudinal components of the spin-one gauge field acquire non-zero mass, which is the same for both components. In addition, a new scalar boson is produced with finite coupling to the massive gauge fields – the Higgs boson.

In the Standard Model of particle physics, besides giving mass to the W and Z gauge bosons, the BEH mechanism also plays a vital role with ensuring consistent ultraviolet behaviour of scattering amplitudes. The Higgs boson with mass 125 GeV guarantees unitarity of high energy collisions involving massive W and Z bosons, with the Higgs boson cancelling terms from the longitudinal component of the W and Z bosons that would otherwise violate perturbative unitarity²³⁻²⁶. It is also essential for the renormalizability of the theory, viz. consistent treatment of ultraviolet divergences which appear in Feynman diagrams involving loops²⁷⁻²⁹.

To understand the BEH mechanism, consider the coupling of the gauge field A_μ to a complex scalar field ϕ via the gauge covariant derivative with coupling constant g , viz. $D_\mu\phi = [\partial_\mu + igA_\mu]\phi$. The scalar field is taken with potential

$$V(\phi) = \frac{1}{2}\mu^2\phi^2 + \frac{1}{4}\lambda\phi^4. \quad (1)$$

Here the self-coupling $\lambda \geq 0$ so the potential has a finite minimum, as required for vacuum stability. If $\mu^2 > 0$ the potential

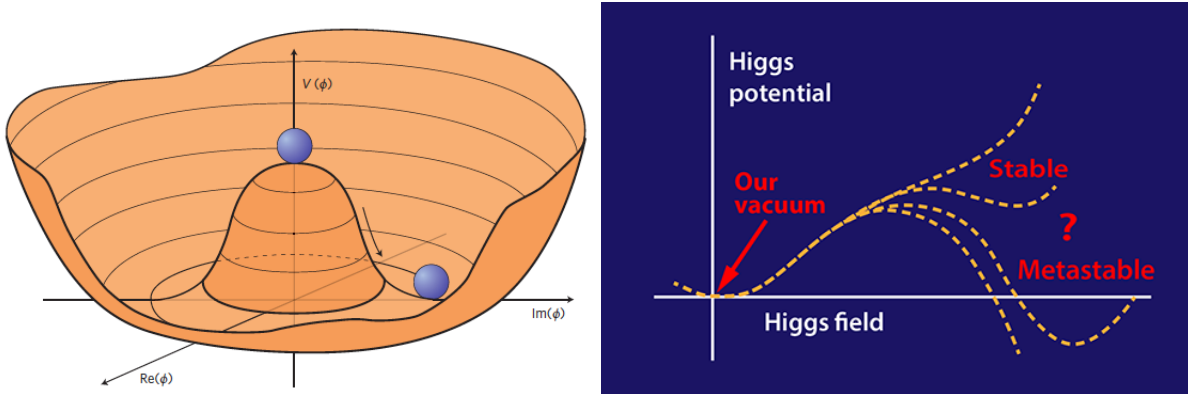


Figure 1. Left: The Higgs potential for $\mu^2 < 0$, Eq. (1). Choosing any of the points at the bottom of the potential spontaneously breaks the rotational U(1) symmetry. Right: Quantum corrections can change the shape of the Higgs potential as discussed in Section 8. Here the minimum of “our vacuum” is taken at $|\phi| = \frac{v}{\sqrt{2}}$. Figure from Ref.³⁰.

describes a particle with mass μ . When $\mu^2 < 0$ the potential has a minimum at

$$|\phi| \equiv \frac{v}{\sqrt{2}} = \sqrt{-\frac{\mu^2}{2\lambda}}. \quad (2)$$

This is illustrated in Fig. 1. Excitations around the degenerate minima of the potential – the bottom of the “Mexican hat” – correspond to a massless Goldstone state. Gauge freedom allows us to choose v as the vacuum expectation value of the real part of ϕ with all choices of vacuum states being degenerate as well as physically equivalent. Expanding the scalar field about this minimum, the Goldstone mode is “eaten” to become the longitudinal mode of A_μ which now acquires mass $g^2 v^2$. The Higgs boson H with mass squared $m_H^2 = 2\lambda v^2$ corresponds to excitations up the rim of the potential.

The issue of massive gauge bosons was first solved by Anderson³¹ in discussion of massive “photons”, called plasmons, in superconductors³¹. The photon behaves as a wave on a sea of BCS Cooper pairs which here act as the scalar field ϕ , condensing in the ground state. The order parameter is not rigid with zero momentum Cooper pairs but fluctuates in the longitudinal component to preserve the translational symmetry of the electron gas. The plasmon’s transverse component is a modification of a real photon propagating in the plasma whereas the longitudinal mode is an attribute of the system. Massive plasmons are manifest through exponential decrease of the magnetic field inside the superconductor (the Meissner effect).

The relativistic case^{17–20} has been introduced to provide a consistent model of weak interactions in particle physics^{32–35}. Contrary to the BCS case, the weak interaction requires the introduction of an additional fundamental scalar field. A dynamic explanation of the Higgs mechanism *à la* BCS would be a major breakthrough and is one of the fundamental motivations to measure with the highest possible precision the properties of the Higgs particle. For a more detailed history of theoretical developments, see Ref.³⁶. For weak interactions the gauge group is SU(2). There are three massless Goldstone modes which combine to form the massive W charged bosons and the massive Z. The massless photon and neutral Z boson are linear combinations of the neutral weak SU(2) gauge boson and a U(1) gauge boson called hypercharge. Within the Standard Model, the BEH mechanism is also important for fermion masses, something required by parity violation of weak interactions³⁷. The weak interaction gauge bosons couple to SU(2) doublets of left-handed leptons and quarks, whereas right-handed fermions are weak interaction neutral. Singlet mass terms for the charged fermions are constructed by contracting the left-handed fermion doublets with the SU(2) Higgs doublet, including the vev, and then multiplying by the right handed fermion. The Standard Model particle masses are

$$m_W^2 = \frac{1}{4}g^2 v^2, \quad m_Z^2 = \frac{1}{4}(g^2 + g'^2)v^2, \quad m_f = y_f \frac{v}{\sqrt{2}}, \quad m_H^2 = 2\lambda v^2. \quad (3)$$

Here g and g' are the SU(2) and U(1) gauge couplings and y_f denotes the fermion Yukawa coupling to the Higgs boson. Before tiny neutrino masses the Standard Model has 18 parameters: 3 gauge couplings and 15 in the Higgs sector (6 quark masses, 3 charged leptons, 4 quark mixing angles including one CP violating complex phase, the W and Higgs masses). There is a wide range of masses with $m_W = 80$ GeV, $m_Z = 91$ GeV, $m_H = 125$ GeV and the charged fermion masses ranging from 0.5 MeV for the electron up to 173 GeV for the top quark.

Small changes in Higgs couplings and particle masses can lead to a very different Universe, assuming that the vacuum remains stable, with one example that small changes in the light-quark masses can prevent Big Bang nucleosynthesis³⁸. Once

radiative corrections are taken into account - see Section 8 - the stability of the Higgs vacuum is very sensitive to the value of the top quark mass. Also and vitally, the Higgs boson cannot be too heavy to do its job with maintaining perturbative unitarity. Indeed, if the Higgs boson had not been found at the LHC new strong dynamics would have been needed in the energy range of the experiments, e.g. involving strongly interacting W^+W^- scattering with the Higgs boson replaced by some broad resonance in the WW system³⁹.

In contrast to particle physics where the Higgs is treated as an elementary particle, in quantum condensed matter systems it forms as a collective mode⁴⁰. Following the Higgs boson discovery in High Energy Physics, collective Higgs states have recently been observed in superconductors⁴¹; for discussion see Refs.^{42,43}. In the particle physics Standard Model one would like to understand deeper the more fundamental origin as well as any internal structure of the Higgs boson.

3 The Higgs boson discovery at CERN and first measurements

The year 2012 was a seminal one for particle physics. More than 40 years after the original postulation for electroweak symmetry breaking via the BEH mechanism, the first potential experimental evidence for the quantum excitation of that field was announced by the ATLAS and CMS experiments on July 4th, at a joint seminar held at CERN, the host of the LHC, and via video connection with the opening session at the international bi-yearly particle physics conference in Melbourne, Australia.

The LHC is an atom smasher that collides proton beams, and has operated at centre of mass energy of 7 and 8 TeV (run 1; 2010-2012) and 13 TeV (run 2; 2015-2018) to search for new particles and phenomena⁴⁴. ATLAS⁴⁵ and CMS⁴⁶ are two general purpose experiments making use of the highest luminosities at the LHC, and are its Higgs hunters.

The expected properties of a Standard Model Higgs boson are theoretically well known for any given – but in 2012 unknown – mass value of this particle. The announcement from ATLAS and CMS was based on the data collected and analysed until then and enough for both experimental collaborations to claim independently the observation of a new particle, i.e. the significance of the result was larger than five standard deviations, or 5σ , away from a background-only result, meaning that the chance of this result being due to a fluctuation of the background is less than 1 in 3,500,000. Measurements which give a significance above 3σ are considered as evidence. A useful quantity extracted from the data is the "signal strength" which is the ratio of the signal rate divided by the predicted rate for a Standard Model Higgs boson at a given mass, and is denoted by the symbol μ_S . The closer μ_S is to one, the more it resembles a Standard Model Higgs boson.

According to the Standard Model, a produced Higgs boson has a lifetime of only $\sim 1.6 \times 10^{-22}$ seconds if its mass is about 125 GeV, after which it disintegrates into particles that are recorded by the experiments. Hence experimenters search for these footprints of the Higgs boson in the detectors. The data showed that the new particle had a mass of around 125 GeV, about 133 times the mass of a proton, and decayed into vector bosons, namely a pair of photons, W bosons, or Z bosons, exactly as anticipated from theory, and therefore got labelled "a Higgs boson candidate". The observed decay into two photons meant that this new particle could not have spin-one, due to the Landau-Yang theorem^{47,48}. The Higgs boson has no electric charge of its own and decays into two photons via a fermion or W boson loop.

The world-wide particle physics community was excited by the announcement, and the international press coverage of the event was huge.

A few months later a next crucial step was made by verifying the quantum properties of this new particle, demonstrating that it had to be a scalar spin-zero particle, as required for the messenger of the BEH field. While some small level mixing with a CP-odd component is still possible, the new particle has been firmly excluded to be a pure CP-odd state⁴⁹⁻⁵¹. This result promoted the particle to be called "a Higgs boson". This still allows that this new particle may not be the Standard Model Higgs boson, but a look-alike, such as a scalar particle from an extended theory sector or even a composite particle. For further insight the Higgs boson properties need to be mapped out in detail which presently can only be done at the LHC. Does this new particle also couple to the other known fundamental particles as expected, i.e. the quarks and charged leptons? What is the exact mass value and width of this resonance? Can we directly measure the shape of the Higgs field potential discussed in Section 2, e.g. via Higgs boson pair production?

ATLAS and CMS discovered this new particle with a data sample of about 10 fb^{-1} each⁵². An additional 15 fb^{-1} was collected by the end of 2012 by both experiments in run 1. From 2015 to 2018, the LHC run 2, the experiments collected 139 fb^{-1} each at a higher center of mass energy: 13 TeV. In the next few years the LHC will deliver for each experiment $\approx 150 \text{ fb}^{-1}$ in run 3 (2022-2024), and then the accelerator and both experiments will be upgraded for the high luminosity phase to collect a total of 3-4 ab^{-1} each.

Many analyses are presently still being finalized on the collected data set but several full run 2 results have been completed and show an emerging picture that we discuss next. In the collisions for this data set about 7 million Higgs bosons have been produced so the LHC can be considered as the first Higgs factory, even though only a fraction can be identified and used to study the properties of the particle. Analyses of data from the LHC go in parallel with advances in precision theoretical calculations for the Standard Model production and decay rates as well as modelling of the backgrounds⁵³⁻⁵⁶.

In the Standard Model all the couplings of the Higgs boson to fermions and vector bosons were known as a function of the Higgs boson's mass before the discovery of the Higgs boson. The only parameter that was not predicted by the theory is the mass of the Higgs boson itself. Upper bounds could be obtained from unitarity in longitudinal vector boson scattering, which was essential in convincing that the LHC should be able to either observe the Higgs boson or signs of new underlying strong dynamics in the TeV range. This is often referred to as the *no-lose* theorem. A 95% confidence level upper bound on the Higgs boson mass of 166 GeV was already derived from previous electroweak measurements, mainly from the former LEP collider at CERN⁵⁷.

To measure the mass of the Higgs boson, decays into a pair of photons or Z bosons, with each Z boson itself decaying into a pair of electrons or muons, are the channels *par excellence*: charged leptons and photons can be measured with excellent precision in the LHC detectors and thus the mass of the Higgs boson can be fully determined from the invariant mass of the final state particles. The resulting distributions show typical resonant structures where the width of the resonance is determined by the detector resolution. The extracted central mass value for the Higgs boson from combined ATLAS and CMS run 1 measurements is reported in Ref.⁵⁸ to be $125.09 \pm 0.21 \pm 0.11$ GeV. Subsequently new values for the mass are reported by CMS of 125.38 ± 0.14 GeV⁵⁹ and by ATLAS of 124.97 ± 0.24 GeV⁶⁰, with these measurements using both the diphoton and ZZ decay channels. It is remarkable that we know the mass of this particle already to almost one per mille precision.

Interestingly, the mass of the Higgs boson at 125 GeV is an "ideal choice" of Nature for a detailed experimental study of this new particle. Indeed the product of the branching ratios of the Standard Model Higgs boson in all decay channels available below the top-antitop threshold has been observed in⁶¹ to be a Gaussian distribution of the Higgs boson mass with a maximum centered at $m_H \approx 125$ GeV, i.e. exactly at the mass value where this new boson has been discovered. No other Standard Model Higgs boson mass value has a better combined signal-strength for the whole set of decay channels. Reversely, this mass value still allows for many Beyond the Standard Model scenarios.

4 The Higgs boson couplings to fermions

The Higgs boson was discovered in channels where it decays to gauge bosons. The observed inclusive production rate of the boson confirmed that the predicted main production process should be through gluon fusion $gg \rightarrow H$. This indirectly implied that the Higgs boson should couple to top quarks, involved in the decay quantum loop. However, direct evidence of the coupling of the Higgs boson to fermions is of paramount importance to demonstrate that the minimal version of the Standard Model initially proposed is correct and that the same scalar field is responsible for the masses of the vector bosons and the charged fermions.

Such a direct test is establishing the decay of the Higgs boson into charged fermions, and was a key physics target for the LHC run 2. Decays to all fermions are kinematically allowed except for the decay into a top anti-top quark pair, but we can still explore the Higgs boson to top quark Yukawa coupling as reported in Section 4.1. An important check is the quantitative comparison of the couplings strengths to the different fermions, which for the quantum particle associated with the BEH field in the Standard Model are expected to be proportional to the masses of the fermions.

The most easily accessible channels are decays to the bottom or b-quarks and to the tau leptons, members of the third and most massive fermion generation. First evidence for decays to the third fermion generation, tau leptons and b-quarks, was reported already with run 1 data. The couplings to the second fermion generation, the muon and the charm and strange quarks, are more challenging. The LHC is unlikely to be able to test couplings to first generation with the present methods at our disposal, and these are targets for a future very intense Higgs factory.

In this Section we next focus on the Higgs boson coupling to the top quark. This is special with the top being heavier than the Higgs boson and with top quark Yukawa coupling to the Higgs boson $y_t \sim 1$. We then discuss measurements of the Higgs boson couplings to the tau lepton, the bottom quark and the lighter mass fermions including a recent experimental highlight: observation of the Higgs boson to muon coupling.

4.1 The Higgs boson to top quark Yukawa coupling

The top quark is the heaviest known fundamental fermion in Nature; its measured mass⁶² of 172.76 ± 0.30 means that the top quark Yukawa coupling is very large, close to one. The precise measurement of this coupling plays an essential role in the energy scale dependence of the Higgs boson self-coupling, which is essential to understanding the stability of the particle physics Higgs vacuum: Does the current vacuum expectation value of the BEH field correspond to the real minimum of the Higgs potential? (For more details, see Section 8.) It also allows for a fundamental check of the quantum consistency of the theory by comparison with indirect measurement through the main gluon fusion production process discussed above, which necessarily proceeds through quantum loop corrections and is therefore potentially sensitive to contributions from other yet unobserved states.

A direct measurement can be made through the associated production of the Higgs boson with a pair of $t\bar{t}$ quarks. The topologies of events are complex and typically contain many jets, among which two at least originate from b-quarks, electrons

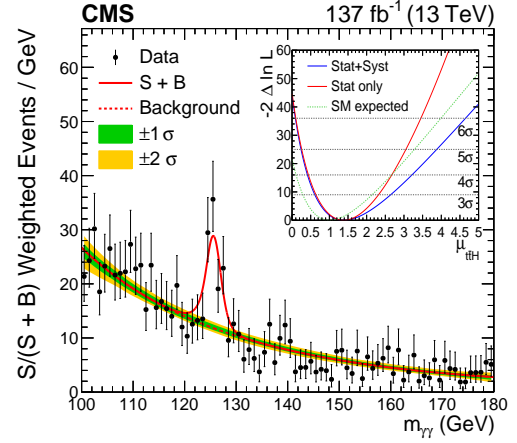
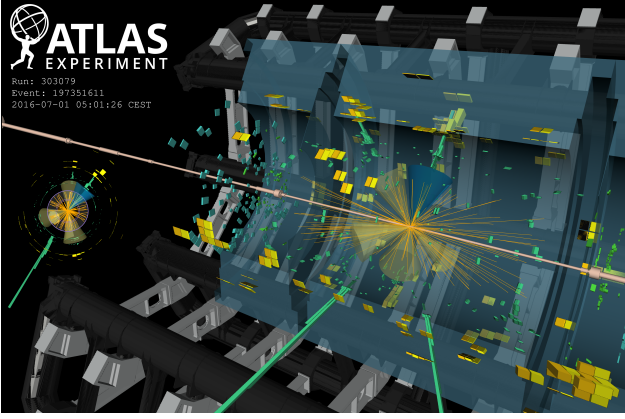


Figure 2. Left: A 3D event display of a candidate $H \rightarrow \gamma\gamma$ in the $pp \rightarrow t\bar{t}H$ production mode, exemplifying the complex topologies of events where in addition of the two isolated photons (in green in the lower part of the detector), 6 jets are present among which one is tagged as originating from a b -quark (blue cone). Right: The distribution of the invariant mass of the diphoton system for events selected in $t\bar{t}H$ specific topologies. The figure also displays the measurement's likelihood as a function of the strength of signal, indicating the subdominant impact of systematic uncertainties in this channel. Figure taken from Ref.⁶⁵

or muons, and the decay products of the Higgs boson itself, see Fig. 2 (left). The first direct observation of the top Yukawa coupling of the Higgs boson was achieved only with a large but partial run 2 dataset and using all Higgs boson decay channels $b\bar{b}$, $\tau^+\tau^-$, WW^* , ZZ^* and $\gamma\gamma$ by ATLAS and CMS^{63,64}. The respective signal strengths for $t\bar{t}H$ production were found to be 1.32 ± 0.39 (ATLAS) and 1.26 ± 0.31 (CMS), in accord with the Standard Model expectation.

With the entire dataset, the diphoton channel alone provides an unambiguous observation of the $pp \rightarrow t\bar{t}H$ production process^{65,66}, see Fig. 2 (right). The other Higgs boson decay channels are more challenging for precision measurements and a key ingredient to improve their sensitivity relies on the progress in the theoretical predictions for the backgrounds.

The presence of the Higgs boson with a large top quark Yukawa coupling can also be indirectly measured through production processes where the Higgs boson does not appear in the final state but contributes as an exchange particle in the intermediate state of the reaction. These indirect measurements have been carried out in top pair production processes, including the spectacular four-top channel for which first evidence has been observed, but are so far not competitive with the constraints from the direct observation of the associated production of a Higgs boson with a top quark pair.

Single top quark production together with a Higgs boson has also been searched for in the experiments. This process is especially interesting⁶⁷ since it is sensitive to the sign of the top quark Yukawa coupling y_t through the tree level interference between the production through the Higgs boson emission by a top quark and a W boson⁶⁸. For Standard Model like couplings of the Higgs boson to W and Z bosons, CMS data⁶⁹ with 36 fb^{-1} favours positive values of y_t and exclude negative values below $-0.9 y_t^{\text{SM}}$. Combined measurements with integrated luminosity of 137 fb^{-1} of $t\bar{t}H$ and tH production in final states with electrons, muons and hadronically decaying tau leptons yield constraints on $\kappa_t = y_t/y_t^{\text{SM}}$ in the range $-0.9 < \kappa_t < -0.7$ or $0.7 < \kappa_t < 1.1$ ⁷⁰.

4.2 The Higgs boson coupling to tau leptons

Tau leptons have a mass of 1.777 GeV and for a Standard Model Higgs boson of 125 GeV the decay rate, or branching ratio, into a $\tau^-\tau^+$ lepton pair is about 6.3%. Tau leptons are unstable, though, and decay with a mean lifetime of about 10^{-13} seconds at the LHC into a narrow low-multiplicity hadronic jet, or a muon or electron, and in all cases in association with one or more neutrinos which go undetected in the experiments. The experiments have developed refined τ -tagging methods in data for the most important τ decay channels, and have also been using additional event activity characteristics apart from the Higgs boson production to master and control the large backgrounds from non-Higgs boson production processes. During run 1 the Higgs boson to $\tau^-\tau^+$ decay was established by both experiments with a significance of about 3σ for CMS and 4.5σ for ATLAS^{71,72} with the 5σ threshold already crossed in run 1 by the ATLAS and CMS combination⁷³.

Recent results based on partial run 2 data confirm these results and have established an observation of the Higgs boson to $\tau^-\tau^+$ decay channel. CMS combined results of several production channels measured with 36 fb^{-1} of data and produced the overall result of an observation of the Higgs boson decaying into a $\tau^-\tau^+$ pair with a significance of 5.5σ and signal strength for a Standard Model Higgs boson μ_S of $1.24 \pm_{0.27}^{0.29}$ from run 2 data⁷⁴ or 0.98 ± 0.18 with a combined significance of 5.9σ

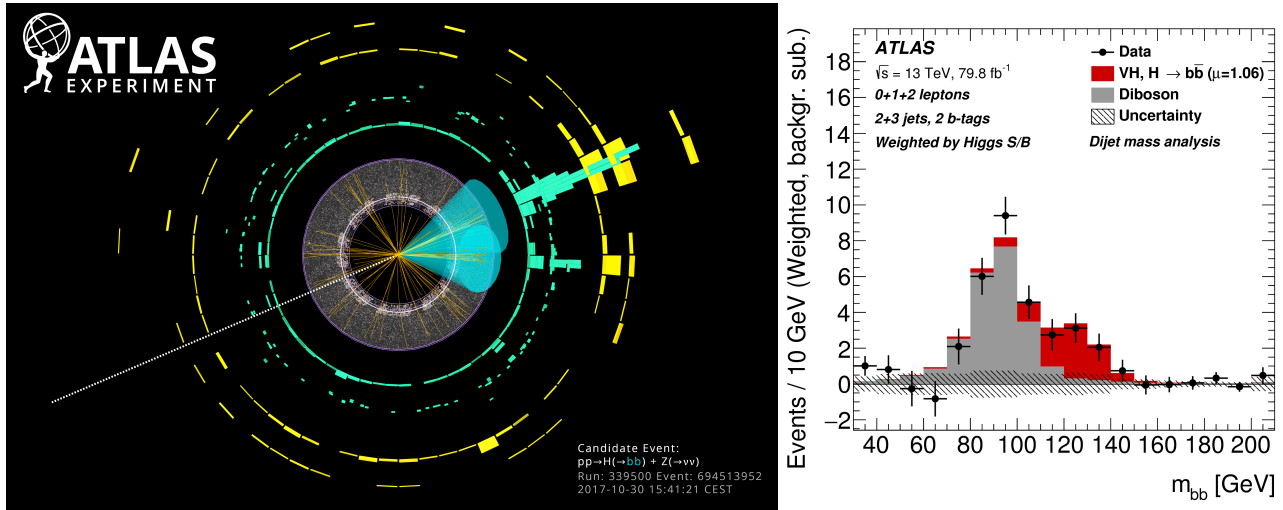


Figure 3. An event display of a candidate $H \rightarrow b\bar{b}$ decay in the plane transverse to the beam axis (left); the cones illustrate the two reconstructed jets of the b-quark decays. The distribution of the m_{bb} invariant mass, showing the $Z \rightarrow b\bar{b}$ (grey) and $H \rightarrow b\bar{b}$ signal (red) signal (right). Figure taken from Ref. ⁷⁷

when both run 1 and run 2 results are included ⁷⁵. The ATLAS result based on 36 fb^{-1} of run 2 data and run 1 results shows a significance of 6.4σ ⁷⁶ and measures a cross section in accord with the 125 GeV Higgs boson prediction. Overall the decay rate for $H \rightarrow \tau^-\tau^+$ is found to be very close to the one expected for a Higgs boson with a mass of 125 GeV.

4.3 The Higgs boson coupling to the bottom quarks

The bottom quark is the heaviest quark accessible in Higgs boson decays, and has a scheme dependent mass of 4.2 GeV ⁶². Free quarks are not observable in Nature. Instead, at the LHC, quarks hadronize in jets of particles resulting from the colour force that connects the produced quarks and breaks-up into colourless hadrons, dominantly mesons. Hadrons containing a b-(anti)quark have short lifetimes, typically around 10^{-12} seconds, and thus cross distances in the detector of typically a few millimeters to centimeters, a feature that can be efficiently explored by the experiments to tag particle jets that contain a b-quark. The branching ratio for a 125 GeV Higgs boson into a b anti-b quark pair is 58% and constitutes the largest Higgs boson decay channel at this mass value. However, the cross sections of b anti-b quarks produced by Standard Model background processes are seven orders of magnitude larger than the Higgs boson production cross section, and hence largely dominate the search regions.

The experimenters have been able to spectacularly reduce these backgrounds by selecting special kinematic regions and by using additional event information, such as additional associated jets and in particular heavy vector W and Z bosons (where the W and Z bosons decay leptonically), to extract the Higgs boson to bottom quark decay signal. In 2018 both experiments announced the observation of this decay channel. ATLAS reported a $H \rightarrow b\bar{b}$ decay signal with 5.4σ and a signal strength of 1.01 ± 0.20 ⁷⁷ based on up to 79.8 fb^{-1} of run 2 and about 25 fb^{-1} run 1 data. CMS observed this channel with 5.6σ significance and a signal strength of 1.04 ± 0.20 ⁷⁸ based on 41.3 fb^{-1} run 2 and about 25 fb^{-1} run 1 data. Hence, the $H \rightarrow b\bar{b}$ decay rate is consistent with the expectations for a 125 GeV Higgs boson. Fig. 3 shows an event display of a candidate $H \rightarrow b\bar{b}$ decay (left), and (right) the distribution of the m_{bb} invariant mass, showing the $Z \rightarrow b\bar{b}$ (grey) and $H \rightarrow b\bar{b}$ signal.

4.4 The Higgs boson coupling to muons

With the Higgs boson decay channels to the third generation fermions, b-quarks and tau leptons, now firmly established the natural next questions is: what about the second generation fermions? Since these particles have lower masses and the signals are often subject to larger backgrounds, extracting these from the data gets increasingly challenging. However these measurements are of uttermost importance to consolidate the scenario of the long-sought BEH mechanism.

The branching ratio of the $H \rightarrow \mu^-\mu^+$ decay in the Standard Model for a Higgs boson of 125 GeV is small, namely 2.18×10^{-4} , but the final state is very simple: it amounts to a search for two oppositely charged muons which have large transverse momenta, of the order of several 10's of GeVs in the laboratory frame, and can be efficiently selected and reconstructed by the experiments. The signal resides on a large background tail: the Z boson to muon pair cross section is 5 orders of magnitude larger than the expected signal.

The hunt for the $H \rightarrow \mu^-\mu^+$ decays started early on. Any observed signal would have unexpected with the initial LHC

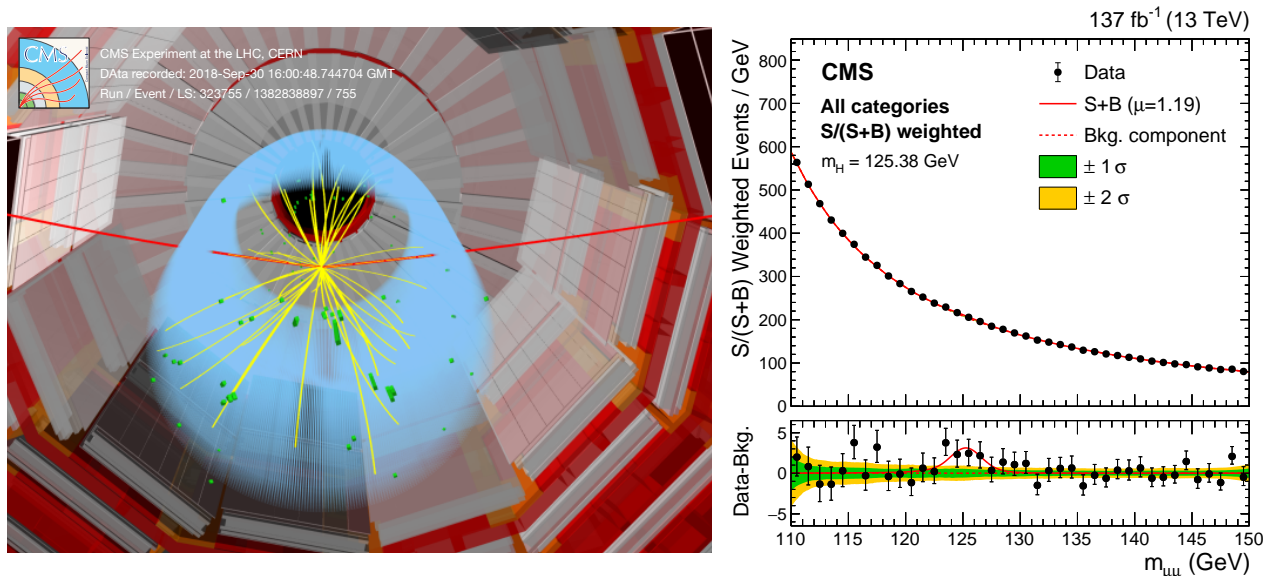


Figure 4. A 3D event display of a candidate $H \rightarrow \mu^- \mu^+$ decay illustrating the reconstructed trajectories of the two muons in red (left); the reconstructed invariant mass of the muon pair is consistent with that of the Higgs boson. The distribution of the $m_{\mu\mu}$ invariant mass, and data – background distribution (right). Figure taken from ⁷⁹.

luminosity since for a true Higgs particle this decay is expected to be strongly suppressed compared to, e.g., the Higgs boson to $\tau^- \tau^*$ decay, and would have been evidence that the newly found particle was *not* the Standard Model Higgs boson! And indeed, no evidence for this decay was found in the run 1 data.

The full set of the run 2 data was recently used by ATLAS and CMS to search for this channel. The large background of mostly Drell-Yan di-muon production required the experiments to use sophisticated tools such as machine learning algorithms to extract a significant signal. In summer 2020, after considerable effort, the experiments were successful and could report for the first time evidence for $H \rightarrow \mu^- \mu^+$ production. CMS reported an observed significance of 3σ and a signal strength of 1.19 ± 0.43 ⁷⁹. ATLAS reported an observed significance of 2σ and a signal strength of 1.2 ± 0.6 ⁸⁰. Fig. 4 shows an event display of a candidate $H \rightarrow \mu^- \mu^+$ decay (left), and (right) the distribution of the $m_{\mu\mu}$ invariant mass.

Clearly, these results open a new research program for the Higgs boson at the LHC: the detailed study of the second fermion generation couplings to the Higgs boson. Presently, the precision of the results is statistics limited, a handicap that will be remedied with the advent of the high luminosity run of the LHC expected to start well before the end of the decade.

4.5 The Higgs boson couplings to lighter quarks

The quarks of the second fermion generation have a scheme dependent mass of 1.27 GeV for the charm quark, c , and a current quark mass of ≈ 90 MeV for the strange quark, s ⁶². The channel $H \rightarrow c\bar{c}$ has a branching ratio of 2.8% for a 125 GeV Higgs boson, a much larger background than for the $H \rightarrow b\bar{b}$ decay channel and a less efficient charm tagger compared to bottom quarks, and as a consequence is far more challenging to observe.

Direct searches for $H \rightarrow c\bar{c}$ have been performed by the experiments, but presently no evidence for this process can be reported, see e.g. ATLAS⁸¹. The most sensitive result to date is an experimental sensitivity of a factor 70 (CMS⁸²) above the predicted Standard Model values. Additional data, improved charm tagging and reconstruction efficiencies, and a deeper use of machine learning techniques will no doubt push these sensitivities closer to the Standard Model observable limits but at this point we cannot yet be sure that this channel will become detectable at the LHC. Other channels are pursued as well, such as $H \rightarrow J/\Psi\gamma$ and $H \rightarrow \Psi(2S)\gamma$, the associated production of the Higgs boson with a c -quark, and the measurement of the charge asymmetry in the associated production mode of a Higgs boson with a vector boson.

The hunt for decays of the Higgs boson to lighter quarks and leptons is even more challenging and is not expected to yield detectable signals for Standard Model Higgs boson couplings at the LHC, but these decays have nevertheless been searched for in topologies such as the di-electron or the VZ and $V\gamma$ decay channels, with V a vector meson.

In all, wherever the LHC presently has sufficient sensitivity, its data dramatically show that the couplings to fermions are in agreement with the expectations of the predictions from the Standard Model BEH mechanism. While the Higgs boson's couplings to light fermions are presently experimentally unknown, it has already been established that these couplings cannot be the same for all generations.

5 Summary of measured Higgs boson's properties

In a few years the LHC will conclude its first phase of operation before a major luminosity upgrade for the machine and experiments is scheduled, but it is already instructive to summarize the overall emerging picture so far on this newly found particle. The experiments have combined measurements of Higgs boson production cross sections and branching fractions. These combinations are based on the analyses of the Higgs boson decay modes $H \rightarrow \gamma\gamma, ZZ, WW, \tau\tau, b\bar{b}, \mu\mu$, searches for decays into invisible final states, and on measurements of off-shell Higgs boson production. Such combinations are made by the experimental collaborations typically after all individual channels have been analysed for a large fraction of the recorded data. ATLAS (CMS) has produced such a combination based using up to 79.8 fb^{-1} (35.9 fb^{-1}) of proton-proton collision data^{83,84} collected in run 2 and found overall global signal strength of the combined fit of all channels to be $\mu_S = 1.11 \pm_{0.08}^{0.09}$ ($\mu_S = 1.17 \pm 0.10$), i.e. close to one, the expected value in the Standard Model. The final combined run 2 analysis based on 139 fb^{-1} from each experiment will probably be available towards the end of 2021.

These results are interpreted in terms of so-called coupling modifiers κ applied to the Standard Model couplings of the Higgs boson to other particles. The coupling modifiers are derived from global fits to all the measurements in different production and decay channels assuming Standard Model relations between the channels, and therefore these κ values do not measure the couplings directly but show levels of deviation from the Standard Model expectations. We can test the coupling-strength scale factors. The result is shown for the different decay channels in Fig. 5 (left) and shows the consistency of the couplings of the Higgs boson to vector bosons and fermions. An overall fit gives $\kappa_V = 1.05 \pm 0.04$ and $\kappa_F = 1.05 \pm 0.09$, i.e. values close to one, the Standard Model prediction. The precision achieved so far in these measurements is not only relying on the excellent performance of the machine and the experiments, but also on the remarkable progress made in the theoretical predictions of the processes at stake, their simulation and their efficient reconstruction.

One of the most prominent achievements to date is measurement of the hierarchy of the relative coupling strengths of the different particles to the Higgs boson! In the Standard Model, the Yukawa coupling between the Higgs boson and the fermions, y_F , is proportional to the fermion masses m_F , while the coupling to weak bosons is proportional to the square of the vector boson masses m_V , with the latter following from the W and Z coupling to the Higgs boson via the Standard Model gauge

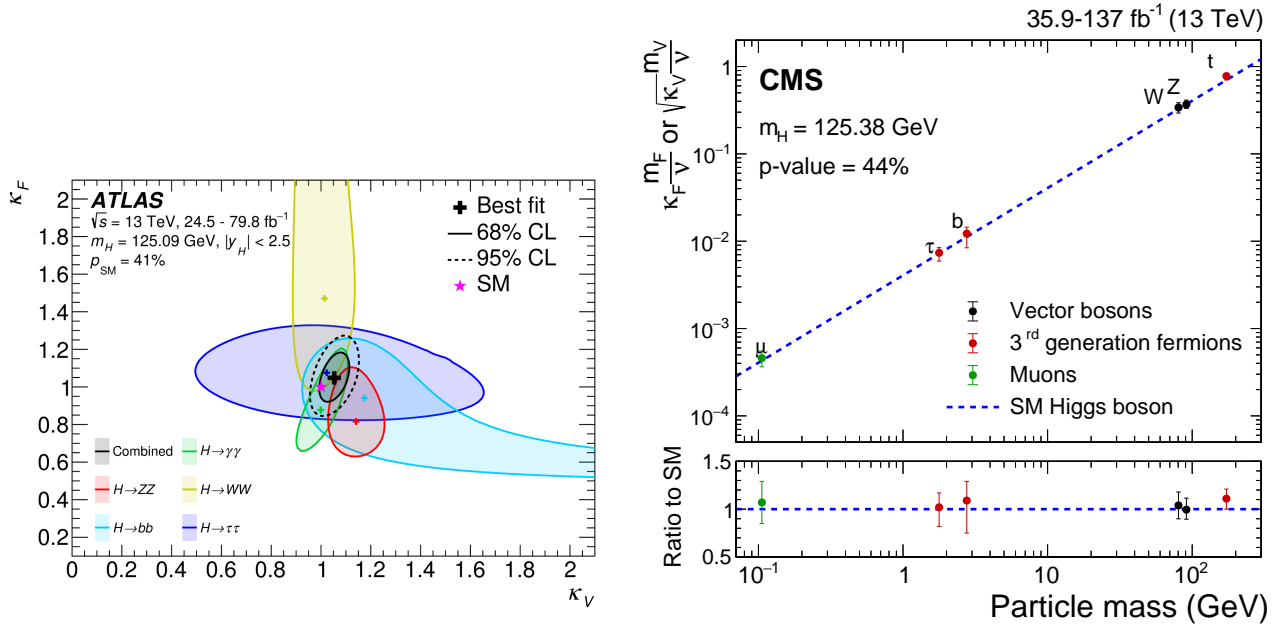


Figure 5. Left: Negative log-likelihood contours at 68% and 95% CL in the (κ_V, κ_F) plane for the individual decay modes and their combination assuming the coupling strengths to fermions and vector bosons to be positive. No contributions from invisible or undetected Higgs boson decays are assumed. The best-fit value for each measurement is indicated by a cross while the Standard Model hypothesis is indicated by a star. Right: the best fit estimates for the reduced coupling modifiers extracted for fermions and weak bosons from the resolved κ -framework compared to their corresponding prediction from the Standard Model. The error bars represent 68% CL intervals for the measured parameters. In the lower panel, the ratios of the measured coupling modifiers values to their Standard Model predictions are shown. Figures taken from Ref.⁸³ and Ref.⁷⁹

covariant derivative⁵⁻⁷. These relations are demonstrated by the data in a dramatic way in Fig. 5 (right). These are the fruits of the first 10 years of data taking and careful analysis at the LHC!

The other landmark result of this first phase of the LHC is the fact that so far no new phenomena beyond those predicted by the Standard Model have been observed. This has led the experiments and the theory communities to perform combined interpretations of all measurements in Higgs, electroweak and top physics in a framework where the Standard Model is considered as an effective field theory^{55,85-89}.

With the full LHC dataset, the precision on the couplings of the Higgs boson is expected to reach between 1% and 2% for the ones to gauge bosons and between 2% and 4% for couplings to the charged fermions of the third generation. Good precision will also be reached for the Higgs boson to muons coupling and to $Z\gamma$ pairs⁹⁰. The final precision for Higgs boson coupling measurements at the LHC in the future will mostly be limited by the precision of theoretical predictions of signal and background processes.

The width of the Higgs particle, which is a measure of its life-time and expected to be 4.1 MeV, cannot be extracted from the observed experimental resonance line shape due to limited experimental resolution of the detectors. Instead an indirect method is used that compares the production rate of the on-mass shell Higgs boson to the production of the Higgs boson far off-mass shell, where it acts as a propagator in the production of a pair of vector bosons (W and Z, both on-mass shell). While the on-mass shell rate depends on the Higgs boson's width, the off-mass shell rates does not and so comparing the rates of the two regimes gives an estimate of the Higgs boson natural width. This method assumes that the running of the Higgs boson couplings do not deviate significantly from those expected from the Standard Model. CMS extracts with 80.2 fb⁻¹ of data a central value of the width to be constrained to $3.2 \pm_{2.2}^{2.8}$ MeV at 68% CL, and a range constrained between [0.08,9.16] MeV at 95% CL⁹¹. The ATLAS experiment reports an upper limit of 14.4 MeV, based on 36 fb⁻¹ of data⁹². It is quite interesting that new results show now also a lower limit of the allowed range, but the measurement is presently still statistics limited. Since the ultimate LHC data sample will have an 20-fold higher statistics, this method is most promising to experimentally verify the Higgs boson's width in the next 15 years. Note however that there is a model dependent assumption using this method that no extra new particles contribute to the off-shell mass rate, i.e. to the rate of Higgs particles with mass larger than 180 GeV, which would invalidate this width extraction.

Pinning down the Higgs boson's width allows us to probe beyond the Standard Model: it accounts for possible invisible decays into particles that do not interact in the detectors, e.g. such as the dark matter candidates discussed in Refs.^{93,94}. In the Standard Model such decays are expected from neutrinos in the final state (from Z boson decays) and are rare, with a branching fraction of approximately 10⁻³. Invisible Higgs boson decays can be directly searched for in event topologies with significant missing transverse momentum. Both ATLAS and CMS have performed searches for these decays in all the main production modes yielding already stringent constraints on the invisible decay width⁹⁵ of ~20%. This can be turned into limits on dark matter searches as shown^{95,96} in Fig. 6. The comparison is performed in the context of Higgs portal models⁹⁷. The translation of the $H \rightarrow$ invisible result into a weak interacting massive particle–nucleon scattering cross section $\sigma_{\text{WIMP-N}}$ relies on an effective field theory approach under the assumption that invisible Higgs boson decays to a pair of WIMPs is kinematically possible and that the WIMP is a scalar or a fermion⁹⁸⁻¹⁰⁰. The excluded $\sigma_{\text{WIMP-N}}$ values range down to e.g. $2 \times 10^{-46} \text{cm}^2$ in the fermion WIMP scenario, probing a new exclusion region for masses below 10 GeV. When extrapolated to the full LHC dataset, including the high luminosity phase, a projected sensitivity of 2.5% should be reached.

6 The Higgs boson self-coupling

In its Standard Model form of Eq.(1), the self coupling λ is related to the Higgs boson's mass and vev, as indicated in Eq. (3), and induces three Higgs and four Higgs boson interaction vertices after the spontaneous breaking of the electroweak symmetry. The measurement of the Higgs boson self interaction is of fundamental importance and the implications of such measurements are discussed in Section 8.

With knowledge of the Higgs boson mass, within the Standard Model the self-coupling of the Higgs boson became known. Its direct measurement is however crucial¹⁰⁶ to understand whether the electroweak symmetry breaking occurs as a crossover, as expected in the Standard Model, or as a strong first order phase transition in the early Universe, which would play a crucial role in our understanding of baryogenesis and has implications for possible gravitational wave signals. It is one of the deepest questions of the Standard Model and may provide a portal to new physics beyond the Standard Model. Experimentally this can be addressed via the measurement of the production of multiple Higgs bosons.

With the run 2 dataset, a major effort to perform complete analyses in a number of final state channels, combining a variety of decay modes for each Higgs boson $\gamma\gamma$, $b\bar{b}$, $\tau^+\tau^-$, WW^* seeking the highest sensitivity to the di-Higgs boson production was made^{107,108}. The final state that was immediately recognized for providing an optimal compromise between the number of events produced and a decent signal-to-background ratio, was $(H \rightarrow b\bar{b})(H \rightarrow \gamma\gamma)$, but adding additional channels can substantially enhance the sensitivity. The net HH production receives contributions from processes that involve Higgs boson self-interactions as well as other interactions that are not sensitive to λ . The measurement of the kinematics of the HH system

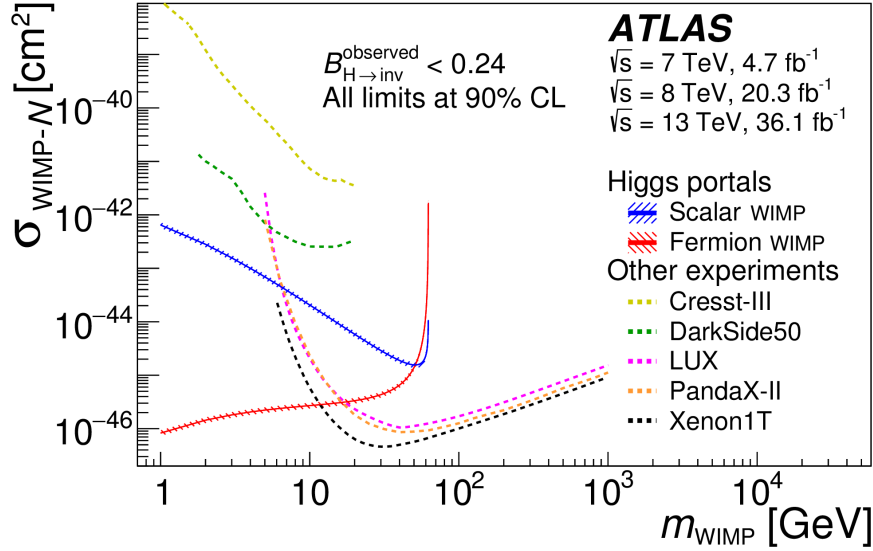


Figure 6. Comparison of the upper limits at 90% CL from direct detection experiments^{101–105} on the spin-independent WIMP-nucleon scattering cross section to the observed exclusion limits, assuming Higgs portal scenarios where the 125 GeV Higgs boson decays to a pair of DM particles⁹⁷. The regions above the limit contours are excluded in the range shown in the plot. Figure taken from Ref.⁹⁶

is crucial to disentangle the different contributions and infer information on λ ¹⁰⁹. Individual experiment combinations with a partial run 2 dataset show that limits below 10 times the Standard Model expected rate can be set on the HH production cross section. An analysis with the full run 2 dataset from CMS in the $b\bar{b}\gamma\gamma$ channel allows one to exclude values of the trilinear coupling smaller than -3.3 and larger than 8.5 times the Standard Model expectation¹¹⁰. With the full run 2 dataset, the ATLAS experiment performed a search for the $HH \rightarrow b\bar{b}b\bar{b}$ final state in the electroweak vector boson fusion production mode¹¹¹, this process has a cross section smaller by approximately one order of magnitude, but is sensitive to $HHVV$ (c_{2V}) coupling and has set a limit of $-1.02 < c_{2V} < 2.71$. The sensitivity of these studies is still far from a measurement of the trilinear coupling. However, it suggests that with the full luminosity for the entire LHC program a combined sensitivity of 4 standard deviations for observing HH production can be obtained⁹⁰. Another possibility is to constrain λ indirectly through its loop level effect on single Higgs boson production¹¹². However, such constraints are model dependent and typically rather weak.

7 Searches for additional Higgs bosons and non Standard Model interactions

While present data suggests the Higgs particle found is very Standard Model-like, the experiments have tried nevertheless to crack and expose it as an imposter, by searching for unexpected Higgs boson production processes or unexpected decays, but without success so far. Is there e.g. more than one Higgs or Higgs-like boson lurking in the wealth of data collected at the LHC? Within the Standard Model only one fundamental scalar is expected, but in many of its extensions the full Higgs family would contain several additional members. Searches for both lighter and more massive (pseudo)-scalar particles, neutral and charged, have been carried out, with no evidence found so far. A recent survey of the searches for additional Higgs bosons is reported in Ref.⁶².

CP-violation is an essential ingredient required for our understanding of the matter anti-matter asymmetry in the Universe. Within the Standard Model very precise electric dipole moment measurements, in particular of the electron¹² measured to be $|d_e/e| < 1.1 \times 10^{-29}$ cm, impose very stringent limits on CP violation in the Higgs Yukawa sector¹¹³. These constraints are model dependent, so probing directly the CP properties of the Higgs boson is mandatory. The Standard Model Higgs boson is CP-even. Non CP-even couplings of the Higgs boson to vector bosons have been searched for in Higgs boson decays to ZZ^* and WW^* ^{91,114} and through production in associated channels^{115,116} using several decay modes. CP-odd couplings to fermions have been searched for both in the decay of the Higgs boson to a pair of tau leptons¹¹⁷ and in the $t\bar{t}H$ production mode with the subsequent decay of the Higgs boson to a pair of photons^{66,118}. No significant CP violating effects have been observed.

In the Standard Model the Yukawa couplings are diagonalized in the mass matrix; there are no off-diagonal terms. There are ways to evade this via effective dimension-6 operators yielding models with off-diagonal Yukawa couplings which are of particular interest as these can break the relation between the masses and the couplings and can generate additional Higgs boson self-coupling terms. These operators describe multi-particle correlations beyond the minimal Standard Model interactions

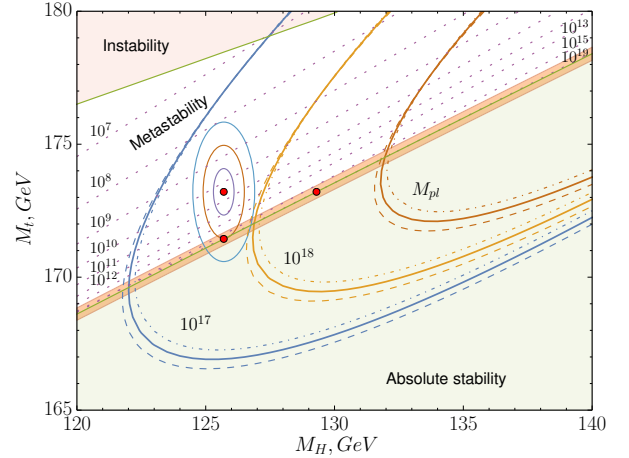
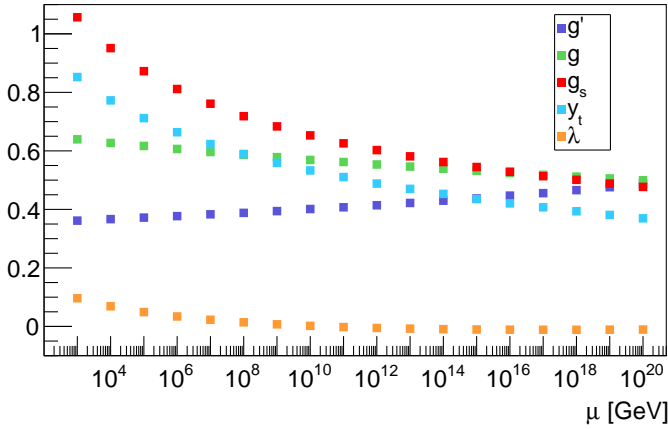


Figure 7. Left: Running of the Standard Model gauge couplings g , g' , g_s for the electroweak SU(2) and U(1) and colour SU(3) interactions, the top quark Yukawa coupling y_t and Higgs boson self-coupling λ . Figure from Ref.¹³¹ with couplings evaluated using the C++ code in Ref.¹³². Right: Phase diagram of vacuum (meta)stability as function of the top quark and Higgs boson masses with one, two and three standard deviations ellipses. The dotted lines refer to the scale where λ touches zero. The parabola-like lines are contours describing the mass parameters leading to vanishing rate of change of λ at fixed large scales. Figure from Ref.¹³³.

and are suppressed by the square of some large mass scale which represents the scale of new physics. The constraints from light quark or lepton flavour changing neutral currents, such as for instance $\mu \rightarrow e\gamma$, are very strong. However in the case of heavier fermions, e.g. from $\tau \rightarrow \mu\gamma$ or $\tau \rightarrow 3\mu$, these are less stringent and the strongest bound on off-diagonal τ - μ Yukawa couplings now comes from the search for Higgs boson decays to a tau-muon pair, with bounds on the mixing term $|Y_{\tau\mu}|$ close to 10^{-3} ^{119,120}. LHC data so far revealed no evidence for higher dimensional operator correlations divided by powers of any large mass scale below the few TeV range^{121,122}.

In the quark sector the existence of the Higgs boson at a mass of around 125 GeV has opened an interesting channel to search for flavour changing neutral current (FCNC) decays of the top quark to a Higgs boson and a charm or an up quark. FCNC top quark decays have been searched for in multiple subsequent Higgs boson decay channels, including the diphoton, WW^* , $\tau^+\tau^-$ and $b\bar{b}$ ¹²³⁻¹²⁹. Bounds on top FCNC decay branching fractions down to approximately 0.2% are reached. These channels complement other FCNC top decays searches with a photon or a Z boson in the final state instead of the Higgs boson.

In summary, the Higgs boson's properties measured at the LHC so far are consistent with the Standard Model expectations within the present measurement precision. Furthermore, with a mass of 125 GeV, the effects of the predicted Higgs boson quantum corrections on electroweak observables within the Standard Model are entirely compatible with the precision measurements carried out at LEP and SLC, and at low energies¹³⁰.

No evidence for additional Higgs bosons, Higgs boson decays into undetected particles, or CP, FCNC or lepton flavour violating effects in Higgs boson decays have been observed yet. These tremendous successes of the Standard Model should however not keep us away from the fundamental open questions which remain unanswered. All these searches will therefore continue with the same vigour with anticipated much larger data sets in the future.

8 Vacuum stability and hierarchies of scales

If taken as the Standard Model Higgs boson, the discovered boson completes Standard Model. It also comes with intriguing observations, including possible clues to new physics. How high in energy might the Standard Model work as our theory of particle interactions, e.g. what is the ultraviolet limit of the Standard Model when taken as an effective theory? What new interactions might lie beyond the Standard Model? Important theoretical issues are the stability of the Higgs vacuum and the small size of the electroweak scale and Higgs boson's mass relative to the Planck scale, 1.2×10^{19} GeV, where quantum gravity effects might apply.

8.1 Vacuum stability

With the discovered boson, the Standard Model is perturbative and predictive when extrapolated to very high energies. Interestingly, if one extrapolates the Standard Model with its measured couplings up to the Planck scale and assumes no

coupling to extra particles or new interactions, then the Higgs vacuum sits very close to the border of stable and metastable^{133–140}, within 1.3 standard deviations of being stable¹³³. With a metastable vacuum there would be a second minimum in the Higgs potential with value low than that measured at our energy scale (as shown in Fig. 1 right) after inclusion of radiative corrections. For an unstable vacuum the BEH potential would become unbounded from below at large values of the BEH field.

Vacuum stability depends on the ultraviolet behaviour of the Higgs boson self-coupling λ . The Standard Model couplings evolve with changing resolution (energy scale) according to the renormalization group as shown in the left panel of Fig. 7. The weak SU(2) and QCD SU(3) couplings, g and g_s are asymptotically free, with $\alpha_i = g_i^2/4\pi$ decaying logarithmically with increasing resolution, whereas the U(1) coupling g' is non asymptotically free, rising in the ultraviolet. The top quark Yukawa coupling y_t decays with increasing resolution. The running of the Higgs boson self-coupling λ determines the stability of the electroweak vacuum. Instability sets in if λ crosses zero deep in the ultraviolet and involves a delicate balance of Standard Model parameters. With the Standard Model parameters measured at the LHC, λ decreases with increasing resolution. This behaviour is dominated by the large Higgs boson coupling to the top quark (and also QCD interactions of the top). Without this coupling, λ would rise in the ultraviolet. In the left panel of Fig. 7 λ crosses zero around 10^{10} GeV with the top quark pole mass $m_t = 173$ GeV and $m_H = 125$ GeV. This signals a metastable vacuum with lifetime greater than about 10^{600} years¹³⁵, very much greater than the present age of the Universe, about 13.8 billion years – see the right panel in Fig. 1. The right panel of Fig. 7 indicates the sensitivity of vacuum stability to small changes in m_t . If the top mass is taken as 171 GeV in these calculations, the vacuum stays stable up to the Planck scale. The measured 125 GeV Higgs boson mass is close to the minimum needed for vacuum stability with the measured top quark mass.

The Standard Model observed in our experiments, assuming no extra particles at higher energies, is strongly correlated with its behaviour in the extreme ultraviolet. Might this be telling us something deep about the origin of the Standard Model?

It is important to emphasise the large extrapolations in these calculations. New physics even at the largest scales can change this picture¹⁴¹. Modulo this caveat, the Higgs vacuum sitting “close to the edge” of stable and metastable suggests possible new critical phenomena in the deep ultraviolet. One possible interpretation is a statistical system in the ultraviolet, near to the Planck scale, close to its critical point^{134,135,140}. As a general rule, theories with new interactions and new particles at higher energies should make the vacuum more stable rather than less!

8.2 Scale hierarchies and the origin of Standard Model gauge symmetries

The Higgs boson’s mass is very much less than the Planck scale despite quantum corrections which naively act to push its mass towards the deep ultraviolet. Under renormalization, the Higgs boson’s mass squared comes with a quadratically divergent counterterm which comes from the Higgs boson self-energy, viz.

$$m_{\text{H bare}}^2 = m_{\text{H ren}}^2 + \delta m_{\text{H}}^2, \quad (4)$$

where

$$\delta m_{\text{H}}^2 = \frac{K^2}{16\pi^2} \frac{6}{v^2} \left(m_{\text{H}}^2 + m_{\text{Z}}^2 + 2m_{\text{W}}^2 - 4m_{\text{t}}^2 \right) \quad (5)$$

relates the renormalized and bare Higgs boson masses and we neglect small contributions from lighter mass quarks. Here K is an ultraviolet cut-off scale on the momentum integrals characterizing the limit to which the Standard Model should work. If K is taken as a physical scale, e.g., the Planck scale, then why is the physical Higgs boson’s mass so small compared to the cut-off? This topic, called the hierarchy or naturalness puzzle, has attracted much theoretical attention^{142,143}. What stabilizes the value of m_{H} ? One possibility is that the Higgs boson’s mass is fine tuned, perhaps through some kind of environment selection and perhaps in connection with vacuum stability of the Standard Model. Alternatively, the Standard Model quantum correction to the Higgs boson’s mass, which is dominated by the top quark contribution, might be cancelled by any new particles that couple to the Higgs boson. However, such particles have so far not been seen in the mass range of the LHC. Likewise, any composite structure to the Higgs boson would soften the ultraviolet divergences but there is no evidence for this in the present data. Searches for extra particles and possible composite structure will continue in the next years with increased luminosity at the LHC.

The Standard Model is a mathematically consistent theory up to the Planck scale but is it also physically complete up to the Planck scale? Some new physics is needed but the scale where it first appears is an open issue. It would be very surprising if there is no new physics below the Planck scale. In the absence of new physics one has the naturalness puzzle, which has inspired much thinking about possible extra particles. Theoretical attempts to resolve this include weakly coupled models with a popular candidate being supersymmetry¹⁴⁴, which if present in Nature would be a new symmetry between bosons and fermions. Strongly coupled models where the Higgs boson is considered as a bound state of new dynamics strong at the weak scale are an alternative solution. Here the “lightness” of the Higgs boson can be explained if the Higgs boson turns out to be a pseudo-Nambu–Goldstone boson. Such models include the so called little Higgs^{145,146}, twin Higgs¹⁴⁷ and partial

compositeness¹⁴⁸ models. For a comprehensive review of these ideas and their phenomenology see Chapter 11 of Ref.⁶², with possible alternatives to an elementary Higgs boson also discussed in Ref.¹⁴⁹. A related issue is the deeper origin of the gauge symmetries of particle physics. Might the electroweak and QCD interactions unify in the ultraviolet within some larger gauge group? The ultimate dream of this approach is unification of the Standard Model forces with gravity close to the Planck scale. With unification one expects the running gauge couplings of the Standard Model to meet in the ultraviolet. They do come close – see Fig. 7 – but without exact crossing. This could be achieved with the addition of supersymmetry, SUSY, at TeV energies¹⁵⁰, which might also provide a dark matter candidate particle. While the simplest SUSY models would have liked a Higgs boson mass close to measured value, the absence of any signal for new SUSY particles in LHC experiments means that these models are now strongly constrained^{8,151–153}. The present status of minimal SUSY model predictions for Higgs boson mass(es) is discussed in Ref.¹⁵⁴. Any new symmetries in the ultraviolet must be strongly broken so they are not seen at the energies of our experiments meaning that there is a trade off: the extra symmetry that might exist at higher energies also comes with a (perhaps large) number of new parameters needing extra explanation.

Modulo the large extrapolations involved and any new particles waiting to be discovered at higher energies, it is interesting not to discard the idea that the Standard Model might work to very high energies close to the Planck scale. In this alternative scenario, it is plausible that the Standard Model might behave as an emergent effective theory with gauge symmetries “dissolving” in the extreme ultraviolet^{140,155–160}. That is, the Standard Model particles including the Higgs and gauge bosons could be the long-range, collective excitations of a statistical system near to its critical point that resides close to the Planck scale¹⁴⁰. Emergent gauge symmetries, where we make symmetry as well as breaking it, are important in quantum many body systems such as high temperature superconductors¹⁶¹, in topological phases of matter¹⁶² and in the low energy limit of the Hubbard model¹⁶³ employed in quantum simulations of gauge theories^{164,165}. Emergent gauge symmetry can arise associated with an infrared fixed point in the renormalization group¹⁶⁶.

Gauge symmetry and renormalizability constrain the global symmetries of the Standard Model at mass dimension four¹⁵⁹. If the Standard Model is an effective theory emerging in the infrared, low-energy global symmetries such as lepton and baryon-number conservation can be broken through additional (non-renormalizable) higher dimensional terms, suppressed by powers of a large mass scale M that characterizes the ultraviolet limit of the effective theory^{140,159,160,167}. The tiny neutrino masses suggested by neutrino oscillation data¹⁶⁸ have a simple interpretation in this picture. If neutrinos with zero electric charge are Majorana particles, meaning they are their own antiparticles, then their masses can be linked to lepton number violation and the dimension five Weinberg operator¹⁶⁹, suppressed by single power of M , involving just the lepton and Higgs fields with $m_\nu \sim \Lambda_{\text{ew}}^2/M$ where $\Lambda_{\text{ew}} = 246$ GeV is the electroweak scale and $M \sim 10^{15}$ GeV. If, instead, neutrinos are Dirac particles with their tiny masses coming from Yukawa couplings to the Higgs field, one then has to ask why these Yukawa couplings are so much suppressed relative to the charged lepton couplings with right-handed neutrinos not participating in electroweak interactions.

9 The Higgs boson and cosmology

The Higgs boson influences many ideas in cosmology, from thinking about the accelerating expansion of the Universe today to processes in the early Universe.

The Higgs potential generates a large vacuum energy contribution to the cosmological constant or vacuum energy density ρ_{vac} , a prime candidate for the dark energy that drives the accelerating expansion of the Universe. Astrophysics experiments¹⁷⁰ tell us that $\rho_{\text{vac}} = (0.002 \text{ eV})^4$. In the Standard Model ρ_{vac} receives contributions from the Higgs and QCD condensates, the zero-point energies of quantum field theory and also a gravitational contribution¹⁷¹. Electroweak and QCD contributions are characterized by scales of 246 GeV and 200 MeV, so what cancels them to give the net cosmological constant scale 0.002 eV? This puzzle has attracted considerable theoretical attention and ideas, see e.g. Refs.^{13,37,171–179}. Present measurements are consistent with a time independent cosmological constant. The next generation of cosmology surveys will look for any time dependence of dark energy, with sensitivity to any variations from a time independent cosmological constant of 10% or more¹⁸⁰.

An intriguing issue is the similar size of the cosmological constant scale 0.002 eV to what we expect for the value of light neutrino masses¹⁸¹. With a finite cosmological constant, there is no solution of Einstein’s equations of General Relativity with constant Minkowski metric $g_{\mu\nu}$. Global space-time translational invariance of the vacuum is broken by a finite cosmological constant¹⁷¹. Motivated by the success of the Standard Model and Special Relativity in our experiments, one might suppose that the vacuum including condensates with finite vevs is space-time translational invariant and that flat space-time is consistent at dimension four. Then, if the Standard Model is treated as an effective theory emergent below a large ultraviolet scale M , the global symmetry might be broken through higher dimensional terms with the electroweak and QCD scales Λ_{ew} and Λ_{qcd} entering the cosmological constant with the scale of the leading term suppressed by Λ_{ew}/M (that is, with vacuum energy density $\rho_{\text{vac}} \sim (\Lambda_{\text{ew}}^2/M)^4$ with one factor of Λ_{ew}^2/M for each dimension of space-time)^{131,182}. How the Higgs potential relates to space-time structure is an important issue for cosmology.

One of the main ideas for understanding the matter-antimatter asymmetry in the Universe involves a possible first order phase transition with the Higgs vev generated in the early Universe^{183,184}. Bubbles with Higgs condensate would be created and expand at the speed of light. This scenario also needs new sources of CP violation beyond the usual Standard Model, with recent ideas discussed in¹⁸⁵ together with an extended Higgs sector, e.g. extra singlet scalar, and quantum tunneling processes in the vacuum called sphalerons that violate baryon number. Evidence of any first order electroweak phase transition might show up in future gravitational wave measurements with LISA, the Laser Interferometer Space Antenna mission of the European Space Agency ESA^{186,187} and the proposed AEDGE experiment¹⁸⁸.

Besides accelerating expansion today, the Universe is commonly believed to have undergone an initial period of exponential expansion called inflation, with factor at least 10^{26} in the first about 10^{-33} seconds¹⁵. Inflation is posited to explain the uniformity with small anisotropies in the Cosmic Microwave Background, CMB. The particle physics of inflation is unknown, though there are many theoretical ideas including where the Higgs boson plays an important role¹⁸⁹⁻¹⁹¹ or where the vev of a possible time dependent extra scalar field interpolates between initial inflation and dark energy today^{172,174,192,193}. Possible extra fundamental scalars also enter in extended theories of gravitation, beyond minimal General Relativity¹⁹⁴. One idea of inflation connects the Higgs boson to gravitation with non-minimal coupling $\xi H^2 R$ where R is the Ricci curvature scalar of General Relativity¹⁸⁹. The parameters of this model can be chosen to reproduce key features of the CMB, the measured scalar spectral index and the tensor-to-scalar ratio.

The Higgs boson may thus play an essential role in the evolution of the Universe from its very beginning to the physics we see in our experiments today!

10 Conclusions: Outlook and future measurements - towards a future Higgs factory

The Higgs boson discovered at the LHC is the first ever observed scalar elementary particle, and we are just at the beginning in understanding what this particle can teach us. Are there maybe other (pseudo)scalars out there? What is their role?

The precision reached on Higgs boson properties so far had not been anticipated. Channels have been measured which were thought to be inaccessible. This extraordinary success is due to several factors: (i) the remarkable operation of the LHC; (ii) the robustness of the experiment; (iii) the improvements in experimental techniques; (iv) the revolutions in the theoretical prediction and simulation of the LHC processes; and (v) the "gift of Nature" that the mass of the Higgs boson be precisely at the cross roads of all possible decay modes.

The found Higgs boson so far behaves very Standard Model like with its couplings to the W and Z gauge bosons, to the third family of charged fermions and to muons from the second family, all consistent with the BEH mechanism of mass generation. But presently we do not yet know why the particle masses have the values as observed in Nature. Furthermore, if the Standard Model is extrapolated up to the Planck scale with the measured Higgs boson and top quark parameters, then the electroweak vacuum sits very close to the border of the stable and metastable regions.

Measurements will be continued with the LHC run 3 starting in 2022, doubling the collision statistics recorded till now, and later with the high luminosity upgrade of the LHC¹⁹⁵ starting before the end of this decade, for a factor 20 increase in the total statistics. These measurements will enable considerable increase in precision on our knowledge of the Higgs boson's couplings to a precision of a few % for many of these, as well to make first measurements of the Higgs boson's self-interaction, as shown in Fig. 8. Along with increased experimental precision, there is also need for more precise theoretical technology⁵⁴ for an optimal extraction of key quantities from the data. Scientists at the LHC secretly hope that the precision measurements will show sooner or later deviations from these predictions, and thus the first cracks in the Standard Model.

The Standard Model is an extraordinary theory, fully consistent up to very high energy scales. We know however that it should not be the whole story. How high in energy will it continue to hold before new physics sets in? Most likely, the Higgs boson will provide us with an essential window to probe this new world beyond the Standard Model.

Beyond the Standard Model searches include looking for any CP violating couplings of the Higgs boson, any extended Higgs sector with possible connections to baryogenesis, possible composite structure to the Higgs boson, which could provide indications of unknown underlying dynamics which could be responsible for the BEH mechanism, as well as any decays to possible dark matter candidates which might explain the mysterious 80% missing mass component in the Universe.

The recent European Particle Physics Strategy update^{197,198} highlights precision studies of the Higgs boson and its interactions as the main priority for the next high-energy collider, with long term options post the LHC luminosity upgrade including a Future Circular Collider^{199,200} (FCC-ee) or CLIC linear e^+e^- collider^{201,202} being considered in context of the future of CERN, with additional e^+e^- collider options being discussed such as the ILC linear collider in Japan²⁰³ and a circular collider CEPC in China²⁰⁴. The circular collider projects also include a proton-proton (FCC-hh) and proton-lepton (FCC-eh) option, typically planned as a next stage following the e^+e^- option. A detailed discussion of the precision that can be reached on Higgs boson property measurements with these different options is reported in⁵⁶, with an example for the FCC facility shown in Fig. 8. Electron-positron colliders cannot reach as high centre of mass energies as proton-proton colliders, but benefit from a much cleaner initial collision state consisting of fundamental particles with well defined energies entering the interactions. In

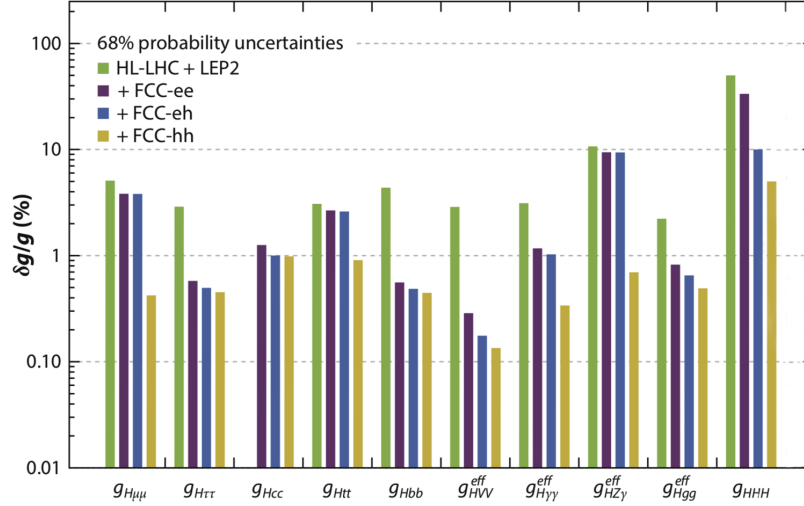


Figure 8. 1σ precision reach at the FCC on the effective Higgs boson couplings to fermions (muons, taus, charm quarks, top quarks and b quarks), to vector bosons (W or Z , photons, $Z\gamma$ and gluons) and the Higgs boson self-coupling in an effective field theory framework. Absolute precision in the electroweak measurements is assumed. The different bars illustrate the improvements that would be possible by combining each FCC stage with the previous knowledge at that time. Abbreviations: FCC, Future Circular Collider; FCC-ee, FCC electron–positron collider; FCC-eh, FCC electron–proton collider; FCC-hh, FCC hadron collider; HL-LHC, High-Luminosity Large Hadron Collider; LEP2, Large Electron–Positron Collider. Figure taken from¹⁹⁶.

particular Higgs production will be measured inclusively from its presence as a recoil to the Z in $e^+e^- \rightarrow HZ$ events, allowing the absolute measurement of the Higgs boson’s coupling to the Z boson.

As shown in Fig. 8 sub-percent precisions on the couplings of the Higgs boson to other gauge bosons and charged fermions of second and third generation, except the strange-quark, can be achieved in e^+e^- collisions where the precision coupling of the Higgs boson to gauge bosons will reach the per mille level, the couplings to bottom-quarks, taus and muons will reach the level of 4 per mille and the coupling to charm-quarks the percent level⁵⁶. In addition, the prospect of measuring, or at least strongly constraining, the couplings to the three lightest quarks and to the electron by dedicated FCC e^+e^- runs at the Higgs boson’s mass, are being evaluated.

The direct measurement of the Yukawa coupling to top quarks requires high-energy proton-proton collisions or higher centre-of-mass energies in e^+e^- and should reach the percent level precision. The study of invisible Higgs boson decays will reach sensitivities well below the percent level and reach the level of the expected Standard Model rate, driven by Higgs bosons decaying in to a pair of Z bosons, which each decay into neutrinos.

To improve significantly on the precision of Higgs boson self-coupling with direct measurements will require high-energy hadron beams, in lepton-hadron or hadron-hadron mode operation, with the highest expected precision of approximately 5% being obtained at a very high-energy proton-proton collider with centre-of-mass energy of 100 TeV⁵⁶.

Besides the charged leptons and quarks, the Higgs boson might also play a key role in generation of neutrino masses, where if neutrinos are their own antiparticles the neutrino mass enters through the dimension-five Weinberg operator. Neutrinoless double β decay experiments aim to look for Majorana neutrinos with the next generation experiments sensitive to the theoretically interesting mass range^{205,206}. The role of the Higgs potential in the vacuum energy density of the Universe is important to understanding the dark energy that drives the accelerating expansion of the Universe. Signals of possible phase transitions in the early Universe, e.g., responsible for baryogenesis, might be manifest in future gravitational wave measurements.

This rich program of experiment and theory promises to shed exciting new insights into the Higgs boson and its vital role in the physics of the Universe!

References

1. Aad, G. *et al.* Observation of a new particle in the search for the Standard Model Higgs boson with the ATLAS detector at the LHC. *Phys. Lett. B* **716**, 1–29, DOI: [10.1016/j.physletb.2012.08.020](https://doi.org/10.1016/j.physletb.2012.08.020) (2012). [1207.7214](https://arxiv.org/abs/1207.7214).
2. Chatrchyan, S. *et al.* Observation of a New Boson at a Mass of 125 GeV with the CMS Experiment at the LHC. *Phys. Lett. B* **716**, 30–61, DOI: [10.1016/j.physletb.2012.08.021](https://doi.org/10.1016/j.physletb.2012.08.021) (2012). [1207.7235](https://arxiv.org/abs/1207.7235).
3. Englert, F. Nobel Lecture: The BEH mechanism and its scalar boson. *Rev. Mod. Phys.* **86**, 843, DOI: [10.1103/RevModPhys.86.843](https://doi.org/10.1103/RevModPhys.86.843) (2014).
4. Higgs, P. W. Nobel Lecture: Evading the Goldstone theorem. *Rev. Mod. Phys.* **86**, 851, DOI: [10.1103/RevModPhys.86.851](https://doi.org/10.1103/RevModPhys.86.851) (2014).
5. Altarelli, G. Collider Physics within the Standard Model: a Primer. (2013). [1303.2842](https://arxiv.org/abs/1303.2842).
6. Pokorski, S. *Gauge Field Theories, 2nd edition* (Cambridge University Press, 2000).
7. Aitchison, I. & Hey, A. *Gauge theories in particle physics: A practical introduction. Vol. 2: Non-Abelian gauge theories: QCD and the electroweak theory* (CRC Press, 2012).
8. Altarelli, G. The Higgs: so simple yet so unnatural. *Phys. Scripta T* **158**, 014011, DOI: [10.1088/0031-8949/2013/T158/014011](https://doi.org/10.1088/0031-8949/2013/T158/014011) (2013). [1308.0545](https://arxiv.org/abs/1308.0545).
9. The electronvolt, eV, is an energy unit used in particle physics corresponding to about 1.6×10^{-19} Joules, with 1 TeV = 10^{12} eV.
10. Hanneke, D., Fogwell, S. & Gabrielse, G. New Measurement of the Electron Magnetic Moment and the Fine Structure Constant. *Phys. Rev. Lett.* **100**, 120801, DOI: [10.1103/PhysRevLett.100.120801](https://doi.org/10.1103/PhysRevLett.100.120801) (2008). [0801.1134](https://arxiv.org/abs/0801.1134).
11. Parker, R. H., Yu, C., Zhong, W., Estey, B. & Müller, H. Measurement of the fine-structure constant as a test of the Standard Model. *Science* **360**, 191, DOI: [10.1126/science.aap7706](https://doi.org/10.1126/science.aap7706) (2018). [1812.04130](https://arxiv.org/abs/1812.04130).
12. Andreev, V. *et al.* Improved limit on the electric dipole moment of the electron. *Nature* **562**, 355–360, DOI: [10.1038/s41586-018-0599-8](https://doi.org/10.1038/s41586-018-0599-8) (2018).
13. Frieman, J., Turner, M. & Huterer, D. Dark Energy and the Accelerating Universe. *Ann. Rev. Astron. Astrophys.* **46**, 385–432, DOI: [10.1146/annurev.astro.46.060407.145243](https://doi.org/10.1146/annurev.astro.46.060407.145243) (2008). [0803.0982](https://arxiv.org/abs/0803.0982).
14. Dine, M. & Kusenko, A. The Origin of the matter - antimatter asymmetry. *Rev. Mod. Phys.* **76**, 1, DOI: [10.1103/RevModPhys.76.1](https://doi.org/10.1103/RevModPhys.76.1) (2003). [hep-ph/0303065](https://arxiv.org/abs/hep-ph/0303065).
15. Baumann, D. & Peiris, H. V. Cosmological Inflation: Theory and Observations. *Adv. Sci. Lett.* **2**, 105–120, DOI: [10.1166/asl.2009.1019](https://doi.org/10.1166/asl.2009.1019) (2009). [0810.3022](https://arxiv.org/abs/0810.3022).
16. Baudis, L. The Search for Dark Matter. *Eur. Rev.* **26**, 70–81, DOI: [10.1017/S1062798717000783](https://doi.org/10.1017/S1062798717000783) (2018). [1801.08128](https://arxiv.org/abs/1801.08128).
17. Higgs, P. W. Broken symmetries, massless particles and gauge fields. *Phys. Lett.* **12**, 132–133, DOI: [10.1016/0031-9163\(64\)91136-9](https://doi.org/10.1016/0031-9163(64)91136-9) (1964).
18. Higgs, P. W. Broken Symmetries and the Masses of Gauge Bosons. *Phys. Rev. Lett.* **13**, 508–509, DOI: [10.1103/PhysRevLett.13.508](https://doi.org/10.1103/PhysRevLett.13.508) (1964).
19. Higgs, P. W. Spontaneous Symmetry Breakdown without Massless Bosons. *Phys. Rev.* **145**, 1156–1163, DOI: [10.1103/PhysRev.145.1156](https://doi.org/10.1103/PhysRev.145.1156) (1966).
20. Englert, F. & Brout, R. Broken Symmetry and the Mass of Gauge Vector Mesons. *Phys. Rev. Lett.* **13**, 321–323, DOI: [10.1103/PhysRevLett.13.321](https://doi.org/10.1103/PhysRevLett.13.321) (1964).
21. Guralnik, G., Hagen, C. & Kibble, T. Global Conservation Laws and Massless Particles. *Phys. Rev. Lett.* **13**, 585–587, DOI: [10.1103/PhysRevLett.13.585](https://doi.org/10.1103/PhysRevLett.13.585) (1964).
22. Kibble, T. Symmetry breaking in nonAbelian gauge theories. *Phys. Rev.* **155**, 1554–1561, DOI: [10.1103/PhysRev.155.1554](https://doi.org/10.1103/PhysRev.155.1554) (1967).
23. Llewellyn Smith, C. High-Energy Behavior and Gauge Symmetry. *Phys. Lett. B* **46**, 233–236, DOI: [10.1016/0370-2693\(73\)90692-8](https://doi.org/10.1016/0370-2693(73)90692-8) (1973).
24. Bell, J. High-energy behavior of tree diagrams in gauge theories. *Nucl. Phys. B* **60**, 427–436, DOI: [10.1016/0550-3213\(73\)90191-0](https://doi.org/10.1016/0550-3213(73)90191-0) (1973).
25. Cornwall, J. M., Levin, D. N. & Tiktopoulos, G. Uniqueness of spontaneously broken gauge theories. *Phys. Rev. Lett.* **30**, 1268–1270, DOI: [10.1103/PhysRevLett.30.1268](https://doi.org/10.1103/PhysRevLett.30.1268) (1973). [Erratum: *Phys.Rev.Lett.* 31, 572 (1973)].

26. Cornwall, J. M., Levin, D. N. & Tiktopoulos, G. Derivation of Gauge Invariance from High-Energy Unitarity Bounds on the s Matrix. *Phys. Rev. D* **10**, 1145, DOI: [10.1103/PhysRevD.10.1145](https://doi.org/10.1103/PhysRevD.10.1145) (1974). [Erratum: *Phys.Rev.D* 11, 972 (1975)].
27. 't Hooft, G. Renormalizable Lagrangians for Massive Yang-Mills Fields. *Nucl. Phys.* **B35**, 167–188, DOI: [10.1016/0550-3213\(71\)90139-8](https://doi.org/10.1016/0550-3213(71)90139-8) (1971).
28. 't Hooft, G. & Veltman, M. J. G. Regularization and Renormalization of Gauge Fields. *Nucl. Phys.* **B44**, 189–213, DOI: [10.1016/0550-3213\(72\)90279-9](https://doi.org/10.1016/0550-3213(72)90279-9) (1972).
29. Veltman, M. J. G. Perturbation theory of massive Yang-Mills fields. *Nucl. Phys.* **B7**, 637–650, DOI: [10.1016/0550-3213\(68\)90197-1](https://doi.org/10.1016/0550-3213(68)90197-1) (1968).
30. Kusenko, A. Are We on the Brink of the Higgs Abyss? *APS Phys.* **8**, 108–110, DOI: [10.1103/Physics.8.108](https://doi.org/10.1103/Physics.8.108) (2015).
31. Anderson, P. W. Plasmons, Gauge Invariance, and Mass. *Phys. Rev.* **130**, 439–442, DOI: [10.1103/PhysRev.130.439](https://doi.org/10.1103/PhysRev.130.439) (1963).
32. Glashow, S. L. Partial Symmetries of Weak Interactions. *Nucl. Phys.* **22**, 579–588, DOI: [10.1016/0029-5582\(61\)90469-2](https://doi.org/10.1016/0029-5582(61)90469-2) (1961).
33. Weinberg, S. A Model of Leptons. *Phys. Rev. Lett.* **19**, 1264–1266, DOI: [10.1103/PhysRevLett.19.1264](https://doi.org/10.1103/PhysRevLett.19.1264) (1967).
34. Salam, A. Weak and Electromagnetic Interactions. *Proceedings of the 8th Nobel symposium, Ed. N. Svartholm, Almqvist and Wiskell, 1968*, Conf. Proc. **C680519**, 367–377 (1968).
35. 't Hooft, G. & Veltman, M. J. G. Regularization and Renormalization of Gauge Fields. *Nucl. Phys.* **B44**, 189–213, DOI: [10.1016/0550-3213\(72\)90279-9](https://doi.org/10.1016/0550-3213(72)90279-9) (1972).
36. Lykken, J. & Spiropulu, M. The Future of the Higgs Boson. *Phys. Today* **66**, 28–33, DOI: [10.1063/PT.3.2212](https://doi.org/10.1063/PT.3.2212) (2013).
37. Veltman, M. J. G. Reflections on the Higgs system. DOI: [10.5170/CERN-1997-005](https://doi.org/10.5170/CERN-1997-005) (1997).
38. Carr, B. J. & Rees, M. The anthropic principle and the structure of the physical world. *Nature* **278**, 605–612, DOI: [10.1038/278605a0](https://doi.org/10.1038/278605a0) (1979).
39. Chanowitz, M. S. The No-Higgs signal: Strong WW scattering at the LHC. *Czech. J. Phys.* **55**, B45–B58, DOI: [10.1007/s10582-005-0006-1](https://doi.org/10.1007/s10582-005-0006-1) (2005). [hep-ph/0412203](https://arxiv.org/abs/hep-ph/0412203).
40. Littlewood, P. B. & Varma, C. M. Amplitude collective modes in superconductors and their coupling to charge-density waves. *Phys. Rev. B* **26**, 4883–4893, DOI: [10.1103/PhysRevB.26.4883](https://doi.org/10.1103/PhysRevB.26.4883) (1982).
41. Sherman, D., Pracht, U. S., Gorshunov, B. *et al.* The Higgs mode in disordered superconductors close to a quantum phase transition. *Nat. Phys.* **11**, 188–197, DOI: [10.1038/nphys3227](https://doi.org/10.1038/nphys3227) (2015).
42. Anderson, P. W. Higgs, Anderson and all that. *Nat. Phys.* **11**, 93, DOI: [10.1038/nphys3247](https://doi.org/10.1038/nphys3247) (2015).
43. Shimano, R. & Tsuji, N. Higgs mode in superconductors. *Annu. Rev. Condens. Matter Phys.* **11**, 103–124, DOI: [10.1146/annurev-conmatphys-031119-050813](https://doi.org/10.1146/annurev-conmatphys-031119-050813) (2020).
44. Bruning, O. S. *et al.* LHC Design Report Vol.1: The LHC Main Ring. DOI: [10.5170/CERN-2004-003-V-1](https://doi.org/10.5170/CERN-2004-003-V-1) (2004).
45. Aad, G. *et al.* The ATLAS Experiment at the CERN Large Hadron Collider. *JINST* **3**, S08003, DOI: [10.1088/1748-0221/3/08/S08003](https://doi.org/10.1088/1748-0221/3/08/S08003) (2008).
46. Chatrchyan, S. *et al.* The CMS Experiment at the CERN LHC. *JINST* **3**, S08004, DOI: [10.1088/1748-0221/3/08/S08004](https://doi.org/10.1088/1748-0221/3/08/S08004) (2008).
47. Landau, L. On the angular momentum of a system of two photons. *Dokl. Akad. Nauk SSSR* **60**, 207–209, DOI: [10.1016/B978-0-08-010586-4.50070-5](https://doi.org/10.1016/B978-0-08-010586-4.50070-5) (1948).
48. Yang, C.-N. Selection Rules for the Dematerialization of a Particle Into Two Photons. *Phys. Rev.* **77**, 242–245, DOI: [10.1103/PhysRev.77.242](https://doi.org/10.1103/PhysRev.77.242) (1950).
49. Chatrchyan, S. *et al.* Study of the Mass and Spin-Parity of the Higgs Boson Candidate Via Its Decays to Z Boson Pairs. *Phys. Rev. Lett.* **110**, 081803, DOI: [10.1103/PhysRevLett.110.081803](https://doi.org/10.1103/PhysRevLett.110.081803) (2013). [1212.6639](https://arxiv.org/abs/1212.6639).
50. Khachatryan, V. *et al.* Constraints on the spin-parity and anomalous HVV couplings of the Higgs boson in proton collisions at 7 and 8 TeV. *Phys. Rev. D* **92**, 012004, DOI: [10.1103/PhysRevD.92.012004](https://doi.org/10.1103/PhysRevD.92.012004) (2015). [1411.3441](https://arxiv.org/abs/1411.3441).
51. Aad, G. *et al.* Evidence for the spin-0 nature of the Higgs boson using ATLAS data. *Phys. Lett. B* **726**, 120–144, DOI: [10.1016/j.physletb.2013.08.026](https://doi.org/10.1016/j.physletb.2013.08.026) (2013). [1307.1432](https://arxiv.org/abs/1307.1432).

52. A fb^{-1} is a unit that quantifies the integrated luminosity. It has the dimension of inverse area, proportional to the amount of proton-proton collisions produced by the LHC collider. One femtobarn $1\text{fb} = 10^{-43}\text{m}^2$. One inverse attobarn $1\text{ab}^{-1} = 10^3\text{fb}^{-1}$. One inverse femtobarn corresponds to approximately 10^{14} proton-proton collisions in the LHC.
53. Dawson, S., Englert, C. & Plehn, T. Higgs Physics: It ain't over till it's over. *Phys. Rept.* **816**, 1–85, DOI: [10.1016/j.physrep.2019.05.001](https://doi.org/10.1016/j.physrep.2019.05.001) (2019). [1808.01324](https://arxiv.org/abs/1808.01324).
54. Heinrich, G. Collider Physics at the Precision Frontier. (2020). [2009.00516](https://arxiv.org/abs/2009.00516).
55. de Florian, D. *et al.* Handbook of LHC Higgs Cross Sections: 4. Deciphering the Nature of the Higgs Sector. **2/2017**, DOI: [10.23731/CYRM-2017-002](https://doi.org/10.23731/CYRM-2017-002) (2016). [1610.07922](https://arxiv.org/abs/1610.07922).
56. de Blas, J. *et al.* Higgs Boson Studies at Future Particle Colliders. *JHEP* **01**, 139, DOI: [10.1007/JHEP01\(2020\)139](https://doi.org/10.1007/JHEP01(2020)139) (2020). [1905.03764](https://arxiv.org/abs/1905.03764).
57. Alcaraz, J. *et al.* A Combination of preliminary electroweak measurements and constraints on the standard model. (2006). [hep-ex/0612034](https://arxiv.org/abs/hep-ex/0612034).
58. Aad, G. *et al.* Combined Measurement of the Higgs Boson Mass in pp Collisions at $\sqrt{s} = 7$ and 8 TeV with the ATLAS and CMS Experiments. *Phys. Rev. Lett.* **114**, 191803, DOI: [10.1103/PhysRevLett.114.191803](https://doi.org/10.1103/PhysRevLett.114.191803) (2015). [1503.07589](https://arxiv.org/abs/1503.07589).
59. Sirunyan, A. M. *et al.* A measurement of the Higgs boson mass in the diphoton decay channel. *Phys. Lett. B* **805**, 135425, DOI: [10.1016/j.physletb.2020.135425](https://doi.org/10.1016/j.physletb.2020.135425) (2020). [2002.06398](https://arxiv.org/abs/2002.06398).
60. Aaboud, M. *et al.* Measurement of the Higgs boson mass in the $H \rightarrow ZZ^* \rightarrow 4\ell$ and $H \rightarrow \gamma\gamma$ channels with $\sqrt{s} = 13$ TeV pp collisions using the ATLAS detector. *Phys. Lett. B* **784**, 345–366, DOI: [10.1016/j.physletb.2018.07.050](https://doi.org/10.1016/j.physletb.2018.07.050) (2018). [1806.00242](https://arxiv.org/abs/1806.00242).
61. d'Enterria, D. On the Gaussian peak of the product of decay probabilities of the standard model Higgs boson at a mass $m_H \sim 125$ GeV. (2012). [1208.1993](https://arxiv.org/abs/1208.1993).
62. Zyla, P. *et al.* Review of Particle Physics. *PTEP* **2020**, 083C01, DOI: [10.1093/ptep/ptaa104](https://doi.org/10.1093/ptep/ptaa104) (2020).
63. Aaboud, M. *et al.* Observation of Higgs boson production in association with a top quark pair at the LHC with the ATLAS detector. *Phys. Lett. B* **784**, 173–191, DOI: [10.1016/j.physletb.2018.07.035](https://doi.org/10.1016/j.physletb.2018.07.035) (2018). [1806.00425](https://arxiv.org/abs/1806.00425).
64. Sirunyan, A. M. *et al.* Observation of $t\bar{t}H$ production. *Phys. Rev. Lett.* **120**, 231801, DOI: [10.1103/PhysRevLett.120.231801](https://doi.org/10.1103/PhysRevLett.120.231801) (2018). [1804.02610](https://arxiv.org/abs/1804.02610).
65. Sirunyan, A. M. *et al.* Measurements of $t\bar{t}H$ Production and the CP Structure of the Yukawa Interaction between the Higgs Boson and Top Quark in the Diphoton Decay Channel. *Phys. Rev. Lett.* **125**, 061801, DOI: [10.1103/PhysRevLett.125.061801](https://doi.org/10.1103/PhysRevLett.125.061801) (2020). [2003.10866](https://arxiv.org/abs/2003.10866).
66. Aad, G. *et al.* CP Properties of Higgs Boson Interactions with Top Quarks in the $t\bar{t}H$ and tH Processes Using $H \rightarrow \gamma\gamma$ with the ATLAS Detector. *Phys. Rev. Lett.* **125**, 061802, DOI: [10.1103/PhysRevLett.125.061802](https://doi.org/10.1103/PhysRevLett.125.061802) (2020). [2004.04545](https://arxiv.org/abs/2004.04545).
67. Barger, V., Hagiwara, K. & Zheng, Y.-J. Probing the Higgs Yukawa coupling to the top quark at the LHC via single top+Higgs production. *Phys. Rev. D* **99**, 031701, DOI: [10.1103/PhysRevD.99.031701](https://doi.org/10.1103/PhysRevD.99.031701) (2019). [1807.00281](https://arxiv.org/abs/1807.00281).
68. Farina, M., Grojean, C., Maltoni, F., Salvioni, E. & Thamm, A. Lifting degeneracies in Higgs couplings using single top production in association with a Higgs boson. *JHEP* **05**, 022, DOI: [10.1007/JHEP05\(2013\)022](https://doi.org/10.1007/JHEP05(2013)022) (2013). [1211.3736](https://arxiv.org/abs/1211.3736).
69. Sirunyan, A. M. *et al.* Search for associated production of a Higgs boson and a single top quark in proton-proton collisions at $\sqrt{s} = 13$ TeV. *Phys. Rev. D* **99**, 092005, DOI: [10.1103/PhysRevD.99.092005](https://doi.org/10.1103/PhysRevD.99.092005) (2019). [1811.09696](https://arxiv.org/abs/1811.09696).
70. Sirunyan, A. M. *et al.* Measurement of the Higgs boson production rate in association with top quarks in final states with electrons, muons, and hadronically decaying tau leptons at $\sqrt{s} = 13$ TeV. (2020). [2011.03652](https://arxiv.org/abs/2011.03652).
71. Chatrchyan, S. *et al.* Evidence for the 125 GeV Higgs boson decaying to a pair of τ leptons. *JHEP* **05**, 104, DOI: [10.1007/JHEP05\(2014\)104](https://doi.org/10.1007/JHEP05(2014)104) (2014). [1401.5041](https://arxiv.org/abs/1401.5041).
72. Aad, G. *et al.* Evidence for the Higgs-boson Yukawa coupling to tau leptons with the ATLAS detector. *JHEP* **04**, 117, DOI: [10.1007/JHEP04\(2015\)117](https://doi.org/10.1007/JHEP04(2015)117) (2015). [1501.04943](https://arxiv.org/abs/1501.04943).
73. Aad, G. *et al.* Measurements of the Higgs boson production and decay rates and constraints on its couplings from a combined ATLAS and CMS analysis of the LHC pp collision data at $\sqrt{s} = 7$ and 8 TeV. *JHEP* **08**, 045, DOI: [10.1007/JHEP08\(2016\)045](https://doi.org/10.1007/JHEP08(2016)045) (2016). [1606.02266](https://arxiv.org/abs/1606.02266).
74. Sirunyan, A. M. *et al.* Search for the associated production of the Higgs boson and a vector boson in proton-proton collisions at $\sqrt{s} = 13$ TeV via Higgs boson decays to τ leptons. *JHEP* **06**, 093, DOI: [10.1007/JHEP06\(2019\)093](https://doi.org/10.1007/JHEP06(2019)093) (2019). [1809.03590](https://arxiv.org/abs/1809.03590).

75. Sirunyan, A. M. *et al.* Observation of the Higgs boson decay to a pair of τ leptons with the CMS detector. *Phys. Lett. B* **779**, 283–316, DOI: [10.1016/j.physletb.2018.02.004](https://doi.org/10.1016/j.physletb.2018.02.004) (2018). [1708.00373](https://arxiv.org/abs/1708.00373).
76. Aaboud, M. *et al.* Cross-section measurements of the Higgs boson decaying into a pair of τ -leptons in proton-proton collisions at $\sqrt{s} = 13$ TeV with the ATLAS detector. *Phys. Rev. D* **99**, 072001, DOI: [10.1103/PhysRevD.99.072001](https://doi.org/10.1103/PhysRevD.99.072001) (2019). [1811.08856](https://arxiv.org/abs/1811.08856).
77. Aaboud, M. *et al.* Observation of $H \rightarrow b\bar{b}$ decays and VH production with the ATLAS detector. *Phys. Lett. B* **786**, 59–86, DOI: [10.1016/j.physletb.2018.09.013](https://doi.org/10.1016/j.physletb.2018.09.013) (2018). [1808.08238](https://arxiv.org/abs/1808.08238).
78. Sirunyan, A. M. *et al.* Observation of Higgs boson decay to bottom quarks. *Phys. Rev. Lett.* **121**, 121801, DOI: [10.1103/PhysRevLett.121.121801](https://doi.org/10.1103/PhysRevLett.121.121801) (2018). [1808.08242](https://arxiv.org/abs/1808.08242).
79. Sirunyan, A. M. *et al.* Evidence for Higgs boson decay to a pair of muons. *JHEP* **01**, 148, DOI: [10.1007/JHEP01\(2021\)148](https://doi.org/10.1007/JHEP01(2021)148) (2021). [2009.04363](https://arxiv.org/abs/2009.04363).
80. Aad, G. *et al.* A search for the dimuon decay of the Standard Model Higgs boson with the ATLAS detector. *Phys. Lett. B* **812**, 135980, DOI: [10.1016/j.physletb.2020.135980](https://doi.org/10.1016/j.physletb.2020.135980) (2021). [2007.07830](https://arxiv.org/abs/2007.07830).
81. Aaboud, M. *et al.* Search for the Decay of the Higgs Boson to Charm Quarks with the ATLAS Experiment. *Phys. Rev. Lett.* **120**, 211802, DOI: [10.1103/PhysRevLett.120.211802](https://doi.org/10.1103/PhysRevLett.120.211802) (2018). [1802.04329](https://arxiv.org/abs/1802.04329).
82. Sirunyan, A. M. *et al.* A search for the standard model Higgs boson decaying to charm quarks. *JHEP* **03**, 131, DOI: [10.1007/JHEP03\(2020\)131](https://doi.org/10.1007/JHEP03(2020)131) (2020). [1912.01662](https://arxiv.org/abs/1912.01662).
83. Aad, G. *et al.* Combined measurements of Higgs boson production and decay using up to 80 fb^{-1} of proton-proton collision data at $\sqrt{s} = 13$ TeV collected with the ATLAS experiment. *Phys. Rev. D* **101**, 012002, DOI: [10.1103/PhysRevD.101.012002](https://doi.org/10.1103/PhysRevD.101.012002) (2020). [1909.02845](https://arxiv.org/abs/1909.02845).
84. Sirunyan, A. M. *et al.* Combined measurements of Higgs boson couplings in proton–proton collisions at $\sqrt{s} = 13$ TeV. *Eur. Phys. J. C* **79**, 421, DOI: [10.1140/epjc/s10052-019-6909-y](https://doi.org/10.1140/epjc/s10052-019-6909-y) (2019). [1809.10733](https://arxiv.org/abs/1809.10733).
85. Giudice, G., Grojean, C., Pomarol, A. & Rattazzi, R. The Strongly-Interacting Light Higgs. *JHEP* **06**, 045, DOI: [10.1088/1126-6708/2007/06/045](https://doi.org/10.1088/1126-6708/2007/06/045) (2007). [hep-ph/0703164](https://arxiv.org/abs/hep-ph/0703164).
86. Grzadkowski, B., Iskrzynski, M., Misiak, M. & Rosiek, J. Dimension-Six Terms in the Standard Model Lagrangian. *JHEP* **10**, 085, DOI: [10.1007/JHEP10\(2010\)085](https://doi.org/10.1007/JHEP10(2010)085) (2010). [1008.4884](https://arxiv.org/abs/1008.4884).
87. Ellis, J., Sanz, V. & You, T. Complete Higgs Sector Constraints on Dimension-6 Operators. *JHEP* **07**, 036, DOI: [10.1007/JHEP07\(2014\)036](https://doi.org/10.1007/JHEP07(2014)036) (2014). [1404.3667](https://arxiv.org/abs/1404.3667).
88. Falkowski, A. & Riva, F. Model-independent precision constraints on dimension-6 operators. *JHEP* **02**, 039, DOI: [10.1007/JHEP02\(2015\)039](https://doi.org/10.1007/JHEP02(2015)039) (2015). [1411.0669](https://arxiv.org/abs/1411.0669).
89. Dawson, S., Homiller, S. & Lane, S. D. Putting standard model EFT fits to work. *Phys. Rev. D* **102**, 055012, DOI: [10.1103/PhysRevD.102.055012](https://doi.org/10.1103/PhysRevD.102.055012) (2020). [2007.01296](https://arxiv.org/abs/2007.01296).
90. Cepeda, M. *et al.* Report from Working Group 2: Higgs Physics at the HL-LHC and HE-LHC. *CERN Yellow Rep. Monogr.* **7**, 221–584, DOI: [10.23731/CYRM-2019-007.221](https://doi.org/10.23731/CYRM-2019-007.221) (2019). [1902.00134](https://arxiv.org/abs/1902.00134).
91. Sirunyan, A. M. *et al.* Measurements of the Higgs boson width and anomalous HVV couplings from on-shell and off-shell production in the four-lepton final state. *Phys. Rev. D* **99**, 112003, DOI: [10.1103/PhysRevD.99.112003](https://doi.org/10.1103/PhysRevD.99.112003) (2019). [1901.00174](https://arxiv.org/abs/1901.00174).
92. Aaboud, M. *et al.* Constraints on off-shell Higgs boson production and the Higgs boson total width in $ZZ \rightarrow 4\ell$ and $ZZ \rightarrow 2\ell 2\nu$ final states with the ATLAS detector. *Phys. Lett. B* **786**, 223–244, DOI: [10.1016/j.physletb.2018.09.048](https://doi.org/10.1016/j.physletb.2018.09.048) (2018). [1808.01191](https://arxiv.org/abs/1808.01191).
93. Arcadi, G., Djouadi, A. & Raidal, M. Dark Matter through the Higgs portal. *Phys. Rept.* **842**, 1–180, DOI: [10.1016/j.physrep.2019.11.003](https://doi.org/10.1016/j.physrep.2019.11.003) (2020). [1903.03616](https://arxiv.org/abs/1903.03616).
94. Carmona, A., Castellano Ruiz, J. & Neubert, M. A warped scalar portal to fermionic dark matter. *Eur. Phys. J. C* **81**, 58, DOI: [10.1140/epjc/s10052-021-08851-0](https://doi.org/10.1140/epjc/s10052-021-08851-0) (2021). [2011.09492](https://arxiv.org/abs/2011.09492).
95. Sirunyan, A. M. *et al.* Search for invisible decays of a Higgs boson produced through vector boson fusion in proton-proton collisions at $\sqrt{s} = 13$ TeV. *Phys. Lett. B* **793**, 520–551, DOI: [10.1016/j.physletb.2019.04.025](https://doi.org/10.1016/j.physletb.2019.04.025) (2019). [1809.05937](https://arxiv.org/abs/1809.05937).
96. Aaboud, M. *et al.* Combination of searches for invisible Higgs boson decays with the ATLAS experiment. *Phys. Rev. Lett.* **122**, 231801, DOI: [10.1103/PhysRevLett.122.231801](https://doi.org/10.1103/PhysRevLett.122.231801) (2019). [1904.05105](https://arxiv.org/abs/1904.05105).

97. Patt, B. & Wilczek, F. Higgs-field portal into hidden sectors. (2006). [hep-ph/0605188](#).
98. Eboli, O. J. & Zeppenfeld, D. Observing an invisible Higgs boson. *Phys. Lett. B* **495**, 147–154, DOI: [10.1016/S0370-2693\(00\)01213-2](#) (2000). [hep-ph/0009158](#).
99. Fox, P. J., Harnik, R., Kopp, J. & Tsai, Y. Missing Energy Signatures of Dark Matter at the LHC. *Phys. Rev. D* **85**, 056011, DOI: [10.1103/PhysRevD.85.056011](#) (2012). [1109.4398](#).
100. De Simone, A., Giudice, G. F. & Strumia, A. Benchmarks for Dark Matter Searches at the LHC. *JHEP* **06**, 081, DOI: [10.1007/JHEP06\(2014\)081](#) (2014). [1402.6287](#).
101. Petricca, F. *et al.* First results on low-mass dark matter from the CRESST-III experiment. *J. Phys. Conf. Ser.* **1342**, 012076, DOI: [10.1088/1742-6596/1342/1/012076](#) (2020). [1711.07692](#).
102. Akerib, D. *et al.* Results from a search for dark matter in the complete LUX exposure. *Phys. Rev. Lett.* **118**, 021303, DOI: [10.1103/PhysRevLett.118.021303](#) (2017). [1608.07648](#).
103. Cui, X. *et al.* Dark Matter Results From 54-Ton-Day Exposure of PandaX-II Experiment. *Phys. Rev. Lett.* **119**, 181302, DOI: [10.1103/PhysRevLett.119.181302](#) (2017). [1708.06917](#).
104. Aprile, E. *et al.* Dark Matter Search Results from a One Ton-Year Exposure of XENON1T. *Phys. Rev. Lett.* **121**, 111302, DOI: [10.1103/PhysRevLett.121.111302](#) (2018). [1805.12562](#).
105. Agnes, P. *et al.* Low-Mass Dark Matter Search with the DarkSide-50 Experiment. *Phys. Rev. Lett.* **121**, 081307, DOI: [10.1103/PhysRevLett.121.081307](#) (2018). [1802.06994](#).
106. Carena, M., Liu, Z. & Riemann, M. Probing the electroweak phase transition via enhanced di-Higgs boson production. *Phys. Rev.* **D97**, 095032, DOI: [10.1103/PhysRevD.97.095032](#) (2018). [1801.00794](#).
107. Aad, G. *et al.* Combination of searches for Higgs boson pairs in pp collisions at $\sqrt{s} = 13$ TeV with the ATLAS detector. *Phys. Lett. B* **800**, 135103, DOI: [10.1016/j.physletb.2019.135103](#) (2020). [1906.02025](#).
108. Sirunyan, A. M. *et al.* Combination of searches for Higgs boson pair production in proton-proton collisions at $\sqrt{s} = 13$ TeV. *Phys. Rev. Lett.* **122**, 121803, DOI: [10.1103/PhysRevLett.122.121803](#) (2019). [1811.09689](#).
109. Alison, J. *et al.* Higgs boson potential at colliders: Status and perspectives. *Rev. Phys.* **5**, 100045, DOI: [10.1016/j.revip.2020.100045](#) (2020). [1910.00012](#).
110. Sirunyan, A. M. *et al.* Search for nonresonant Higgs boson pair production in final states with two bottom quarks and two photons in proton-proton collisions at $\sqrt{s} = 13$ TeV. (2020). [2011.12373](#).
111. Aad, G. *et al.* Search for the $HH \rightarrow b\bar{b}b\bar{b}$ process via vector-boson fusion production using proton-proton collisions at $\sqrt{s} = 13$ TeV with the ATLAS detector. *JHEP* **07**, 108, DOI: [10.1007/JHEP07\(2020\)108](#) (2020). [Erratum: *JHEP* **01**, 145 (2021)], [2001.05178](#).
112. Di Vita, S., Grojean, C., Panico, G., Riemann, M. & Vantalon, T. A global view on the Higgs self-coupling. *JHEP* **09**, 069, DOI: [10.1007/JHEP09\(2017\)069](#) (2017). [1704.01953](#).
113. Brod, J., Haisch, U. & Zupan, J. Constraints on CP-violating Higgs couplings to the third generation. *JHEP* **11**, 180, DOI: [10.1007/JHEP11\(2013\)180](#) (2013). [1310.1385](#).
114. Aaboud, M. *et al.* Measurement of the Higgs boson coupling properties in the $H \rightarrow ZZ^* \rightarrow 4\ell$ decay channel at $\sqrt{s} = 13$ TeV with the ATLAS detector. *JHEP* **03**, 095, DOI: [10.1007/JHEP03\(2018\)095](#) (2018). [1712.02304](#).
115. Aad, G. *et al.* Test of CP Invariance in vector-boson fusion production of the Higgs boson using the Optimal Observable method in the ditau decay channel with the ATLAS detector. *Eur. Phys. J. C* **76**, 658, DOI: [10.1140/epjc/s10052-016-4499-5](#) (2016). [1602.04516](#).
116. Sirunyan, A. M. *et al.* Constraints on anomalous HVV couplings from the production of Higgs bosons decaying to τ lepton pairs. *Phys. Rev. D* **100**, 112002, DOI: [10.1103/PhysRevD.100.112002](#) (2019). [1903.06973](#).
117. Berge, S., Bernreuther, W., Niepelt, B. & Spiesberger, H. How to pin down the CP quantum numbers of a Higgs boson in its tau decays at the LHC. *Phys. Rev. D* **84**, 116003, DOI: [10.1103/PhysRevD.84.116003](#) (2011). [1108.0670](#).
118. Sirunyan, A. M. *et al.* Search for production of four top quarks in final states with same-sign or multiple leptons in proton-proton collisions at $\sqrt{s} = 13$ TeV. *Eur. Phys. J. C* **80**, 75, DOI: [10.1140/epjc/s10052-019-7593-7](#) (2020). [1908.06463](#).
119. Aad, G. *et al.* Searches for lepton-flavour-violating decays of the Higgs boson in $\sqrt{s} = 13$ TeV pp collisions with the ATLAS detector. *Phys. Lett. B* **800**, 135069, DOI: [10.1016/j.physletb.2019.135069](#) (2020). [1907.06131](#).

120. Sirunyan, A. M. *et al.* Search for lepton flavour violating decays of the Higgs boson to $\mu\tau$ and $e\tau$ in proton-proton collisions at $\sqrt{s} = 13$ TeV. *JHEP* **06**, 001, DOI: [10.1007/JHEP06\(2018\)001](https://doi.org/10.1007/JHEP06(2018)001) (2018). [1712.07173](https://arxiv.org/abs/1712.07173).
121. Slade, E. Towards global fits in EFT's and New Physics implications. *PoS LHCP2019*, 150, DOI: [10.22323/1.350.0150](https://doi.org/10.22323/1.350.0150) (2019). [1906.10631](https://arxiv.org/abs/1906.10631).
122. Ellis, J., Madigan, M., Mimasu, K., Sanz, V. & You, T. Top, Higgs, Diboson and Electroweak Fit to the Standard Model Effective Field Theory. (2020). [2012.02779](https://arxiv.org/abs/2012.02779).
123. ATLAS Collaboration. Search for top quark decays $t \rightarrow qH$ with $H \rightarrow \gamma\gamma$ using the ATLAS detector. *JHEP* **06**, 008, DOI: [10.1007/JHEP06\(2014\)008](https://doi.org/10.1007/JHEP06(2014)008) (2014). [1403.6293](https://arxiv.org/abs/1403.6293).
124. ATLAS Collaboration. Search for flavour-changing neutral current top quark decays $t \rightarrow Hq$ in pp collisions at $\sqrt{s} = 8$ TeV with the ATLAS detector. *JHEP* **12**, 061, DOI: [10.1007/JHEP12\(2015\)061](https://doi.org/10.1007/JHEP12(2015)061) (2015). [1509.06047](https://arxiv.org/abs/1509.06047).
125. ATLAS Collaboration. Search for top quark decays $t \rightarrow qH$, with $H \rightarrow \gamma\gamma$, in $\sqrt{s} = 13$ TeV pp collisions using the ATLAS detector. *JHEP* **10**, 129, DOI: [10.1007/JHEP10\(2017\)129](https://doi.org/10.1007/JHEP10(2017)129) (2017). [1707.01404](https://arxiv.org/abs/1707.01404).
126. ATLAS Collaboration. Search for flavor-changing neutral currents in top quark decays $t \rightarrow Hc$ and $t \rightarrow Hu$ in multilepton final states in proton-proton collisions at $\sqrt{s} = 13$ TeV with the ATLAS detector. *Phys. Rev. D* **98**, 032002, DOI: [10.1103/PhysRevD.98.032002](https://doi.org/10.1103/PhysRevD.98.032002) (2018). [1805.03483](https://arxiv.org/abs/1805.03483).
127. ATLAS Collaboration. Search for top-quark decays $t \rightarrow Hq$ with 36 fb^{-1} of pp collision data at $\sqrt{s} = 13$ TeV with the ATLAS detector. *JHEP* **05**, 123, DOI: [10.1007/JHEP05\(2019\)123](https://doi.org/10.1007/JHEP05(2019)123) (2019). [1812.11568](https://arxiv.org/abs/1812.11568).
128. CMS Collaboration. Search for top quark decays via Higgs-boson-mediated flavor-changing neutral currents in pp collisions at $\sqrt{s} = 8$ TeV. *JHEP* **02**, 079, DOI: [10.1007/JHEP02\(2017\)079](https://doi.org/10.1007/JHEP02(2017)079) (2017). [1610.04857](https://arxiv.org/abs/1610.04857).
129. CMS Collaboration. Search for the flavor-changing neutral current interactions of the top quark and the Higgs boson which decays into a pair of b quarks at $\sqrt{s} = 13$ TeV. *JHEP* **06**, 102, DOI: [10.1007/JHEP06\(2018\)102](https://doi.org/10.1007/JHEP06(2018)102) (2018). [1712.02399](https://arxiv.org/abs/1712.02399).
130. Baak, M. Review of electroweak fits of the SM and beyond, after the Higgs discovery – with Gfitter. *PoS EPS-HEP2013*, 203, DOI: [10.22323/1.180.0203](https://doi.org/10.22323/1.180.0203) (2013).
131. Bass, S. D. & Krzysiak, J. The cosmological constant and Higgs mass with emergent gauge symmetries. *Acta Phys. Polon. B* **51**, 1251, DOI: [10.5506/APhysPolB.51.1251](https://doi.org/10.5506/APhysPolB.51.1251) (2020). [2004.05489](https://arxiv.org/abs/2004.05489).
132. Kniehl, B. A., Pikelner, A. F. & Veretin, O. L. mr: a C++ library for the matching and running of the Standard Model parameters. *Comput. Phys. Commun.* **206**, 84–96, DOI: [10.1016/j.cpc.2016.04.017](https://doi.org/10.1016/j.cpc.2016.04.017) (2016). [1601.08143](https://arxiv.org/abs/1601.08143).
133. Bednyakov, A., Kniehl, B., Pikelner, A. & Veretin, O. Stability of the Electroweak Vacuum: Gauge Independence and Advanced Precision. *Phys. Rev. Lett.* **115**, 201802, DOI: [10.1103/PhysRevLett.115.201802](https://doi.org/10.1103/PhysRevLett.115.201802) (2015). [1507.08833](https://arxiv.org/abs/1507.08833).
134. Degrandi, G. *et al.* Higgs mass and vacuum stability in the Standard Model at NNLO. *JHEP* **08**, 098, DOI: [10.1007/JHEP08\(2012\)098](https://doi.org/10.1007/JHEP08(2012)098) (2012). [1205.6497](https://arxiv.org/abs/1205.6497).
135. Buttazzo, D. *et al.* Investigating the near-criticality of the Higgs boson. *JHEP* **12**, 089, DOI: [10.1007/JHEP12\(2013\)089](https://doi.org/10.1007/JHEP12(2013)089) (2013). [1307.3536](https://arxiv.org/abs/1307.3536).
136. Bezrukov, F., Kalmykov, M. Yu., Kniehl, B. A. & Shaposhnikov, M. Higgs Boson Mass and New Physics. *JHEP* **10**, 140, DOI: [10.1007/JHEP10\(2012\)140](https://doi.org/10.1007/JHEP10(2012)140) (2012). [1205.2893](https://arxiv.org/abs/1205.2893).
137. Alekhin, S., Djouadi, A. & Moch, S. The top quark and Higgs boson masses and the stability of the electroweak vacuum. *Phys. Lett.* **B716**, 214–219, DOI: [10.1016/j.physletb.2012.08.024](https://doi.org/10.1016/j.physletb.2012.08.024) (2012). [1207.0980](https://arxiv.org/abs/1207.0980).
138. Masina, I. Higgs boson and top quark masses as tests of electroweak vacuum stability. *Phys. Rev.* **D87**, 053001, DOI: [10.1103/PhysRevD.87.053001](https://doi.org/10.1103/PhysRevD.87.053001) (2013). [1209.0393](https://arxiv.org/abs/1209.0393).
139. Hamada, Y., Kawai, H. & Oda, K.-y. Bare Higgs mass at Planck scale. *Phys. Rev. D* **87**, 053009, DOI: [10.1103/PhysRevD.87.053009](https://doi.org/10.1103/PhysRevD.87.053009) (2013). [Erratum: *Phys.Rev.D* 89, 059901 (2014)], [1210.2538](https://arxiv.org/abs/1210.2538).
140. Jegerlehner, F. The Standard model as a low-energy effective theory: what is triggering the Higgs mechanism? *Acta Phys. Polon. B* **45**, 1167, DOI: [10.5506/APhysPolB.45.1167](https://doi.org/10.5506/APhysPolB.45.1167) (2014). [1304.7813](https://arxiv.org/abs/1304.7813).
141. Branchina, V. & Messina, E. Stability, Higgs Boson Mass and New Physics. *Phys. Rev. Lett.* **111**, 241801, DOI: [10.1103/PhysRevLett.111.241801](https://doi.org/10.1103/PhysRevLett.111.241801) (2013). [1307.5193](https://arxiv.org/abs/1307.5193).
142. Giudice, G. F. Naturally Speaking: The Naturalness Criterion and Physics at the LHC. 155–178, DOI: [10.1142/9789812779762_0010](https://doi.org/10.1142/9789812779762_0010) (2008). [0801.2562](https://arxiv.org/abs/0801.2562).

143. Wells, J. D. Lectures on Higgs Boson Physics in the Standard Model and Beyond. In *39th British Universities Summer School in Theoretical Elementary Particle Physics (BUSSTEPP 2009) Liverpool, United Kingdom, August 24-September 4, 2009* (2009). [0909.4541](#).
144. Wess, J. & Zumino, B. A Lagrangian Model Invariant Under Supergauge Transformations. *Phys. Lett.* **49B**, 52, DOI: [10.1016/0370-2693\(74\)90578-4](#) (1974).
145. Arkani-Hamed, N., Cohen, A. G. & Georgi, H. Electroweak symmetry breaking from dimensional deconstruction. *Phys. Lett. B* **513**, 232–240, DOI: [10.1016/S0370-2693\(01\)00741-9](#) (2001). [hep-ph/0105239](#).
146. Arkani-Hamed, N., Cohen, A. G., Katz, E. & Nelson, A. E. The Lightest Higgs. *JHEP* **07**, 034, DOI: [10.1088/1126-6708/2002/07/034](#) (2002). [hep-ph/0206021](#).
147. Chacko, Z., Goh, H.-S. & Harnik, R. The Twin Higgs: Natural electroweak breaking from mirror symmetry. *Phys. Rev. Lett.* **96**, 231802, DOI: [10.1103/PhysRevLett.96.231802](#) (2006). [hep-ph/0506256](#).
148. Kaplan, D. B. Flavor at SSC energies: A New mechanism for dynamically generated fermion masses. *Nucl. Phys. B* **365**, 259–278, DOI: [10.1016/S0550-3213\(05\)80021-5](#) (1991).
149. Csaki, C., Grojean, C. & Terning, J. Alternatives to an Elementary Higgs. *Rev. Mod. Phys.* **88**, 045001, DOI: [10.1103/RevModPhys.88.045001](#) (2016). [1512.00468](#).
150. Ross, G. G. & Roberts, R. G. Minimal supersymmetric unification predictions. *Nucl. Phys.* **B377**, 571–592, DOI: [10.1016/0550-3213\(92\)90302-R](#) (1992).
151. Altarelli, G. The Higgs and the Excessive Success of the Standard Model. *Frascati Phys. Ser.* **58**, 102 (2014). [1407.2122](#).
152. Pokorski, S. Physics Beyond the Standard Model in Hadronic Collisions. *Acta Phys. Polon. B* **47**, 1767, DOI: [10.5506/APhysPolB.47.1767](#) (2016).
153. Ross, G. G. SUSY: Quo Vadis? *Eur. Phys. J. C* **74**, 2699, DOI: [10.1140/epjc/s10052-013-2699-9](#) (2014).
154. Slavich, P. *et al.* Higgs-mass predictions in the MSSM and beyond. (2020). [2012.15629](#).
155. Jegerlehner, F. The 'Ether world' and elementary particles. In *Theory of elementary particles. Proceedings, 31st International Symposium Ahrenshoop, Buckow, Germany, September 2-6, 1997*, 386–392 (1998). [hep-th/9803021](#).
156. Bjorken, J. Emergent gauge bosons. In *Proceedings to the workshops: What comes beyond the standard model 2000, 2001. Volume 1* (2001). [hep-th/0111196](#).
157. Forster, D., Nielsen, H. B. & Ninomiya, M. Dynamical Stability of Local Gauge Symmetry: Creation of Light from Chaos. *Phys. Lett.* **94B**, 135–140, DOI: [10.1016/0370-2693\(80\)90842-4](#) (1980).
158. Giudice, G. F. The Dawn of the Post-Naturalness Era. In Levy, A., Forte, S. & Ridolfi, G. (eds.) *From My Vast Repertoire ...: Guido Altarelli's Legacy*, 267–292, DOI: [10.1142/9789813238053_0013](#) (2019). [1710.07663](#).
159. Witten, E. Symmetry and Emergence. *Nat. Phys.* **14**, 116–119, DOI: [10.1038/nphys4348](#) (2018). [1710.01791](#).
160. Bass, S. D. Emergent Gauge Symmetries and Particle Physics. *Prog. Part. Nucl. Phys.* **113**, 103756, DOI: [10.1016/j.pnpnp.2020.103756](#) (2020). [2001.01705](#).
161. Baskaran, G. & Anderson, P. W. Gauge theory of high temperature superconductors and strongly correlated Fermi systems. *Phys. Rev.* **B37**, 580–583, DOI: [10.1103/PhysRevB.37.580](#) (1988).
162. Sachdev, S. Topological order, emergent gauge fields, and Fermi surface reconstruction. *Rept. Prog. Phys.* **82**, 014001, DOI: [10.1088/1361-6633/aae110](#) (2019). [1801.01125](#).
163. Affleck, I., Zou, Z., Hsu, T. & Anderson, P. W. SU(2) gauge symmetry of the large-U limit of the Hubbard model. *Phys. Rev.* **B38**, 745–747, DOI: [10.1103/PhysRevB.38.745](#) (1988).
164. Banerjee, D. *et al.* Atomic Quantum Simulation of Dynamical Gauge Fields coupled to Fermionic Matter: From String Breaking to Evolution after a Quench. *Phys. Rev. Lett.* **109**, 175302, DOI: [10.1103/PhysRevLett.109.175302](#) (2012). [1205.6366](#).
165. Bañuls, M. C. *et al.* Simulating Lattice Gauge Theories within Quantum Technologies. *Eur. Phys. J. D* **74**, 165, DOI: [10.1140/epjd/e2020-100571-8](#) (2020). [1911.00003](#).
166. Wetterich, C. Gauge symmetry from decoupling. *Nucl. Phys. B* **915**, 135–167, DOI: [10.1016/j.nuclphysb.2016.12.008](#) (2017). [1608.01515](#).
167. Weinberg, S. Essay: Half a Century of the Standard Model. *Phys. Rev. Lett.* **121**, 220001, DOI: [10.1103/PhysRevLett.121.220001](#) (2018).

168. Baha Balantekin, A. & Kayser, B. On the Properties of Neutrinos. *Ann. Rev. Nucl. Part. Sci.* **68**, 313–338, DOI: [10.1146/annurev-nucl-101916-123044](https://doi.org/10.1146/annurev-nucl-101916-123044) (2018). [1805.00922](https://arxiv.org/abs/1805.00922).
169. Weinberg, S. Baryon and Lepton Nonconserving Processes. *Phys. Rev. Lett.* **43**, 1566–1570, DOI: [10.1103/PhysRevLett.43.1566](https://doi.org/10.1103/PhysRevLett.43.1566) (1979).
170. Aghanim, N. *et al.* Planck 2018 results. VI. Cosmological parameters. *Astron. Astrophys.* **641**, A6, DOI: [10.1051/0004-6361/201833910](https://doi.org/10.1051/0004-6361/201833910) (2020). [1807.06209](https://arxiv.org/abs/1807.06209).
171. Weinberg, S. The Cosmological Constant Problem. *Rev. Mod. Phys.* **61**, 1–23, DOI: [10.1103/RevModPhys.61.1](https://doi.org/10.1103/RevModPhys.61.1) (1989).
172. Wetterich, C. The Cosmon model for an asymptotically vanishing time dependent cosmological 'constant'. *Astron. Astrophys.* **301**, 321–328 (1995). [hep-th/9408025](https://arxiv.org/abs/hep-th/9408025).
173. Sahni, V. & Starobinsky, A. A. The Case for a positive cosmological Lambda term. *Int. J. Mod. Phys. D9*, 373–444, DOI: [10.1142/S0218271800000542](https://doi.org/10.1142/S0218271800000542) (2000). [astro-ph/9904398](https://arxiv.org/abs/astro-ph/9904398).
174. Peebles, P. J. E. & Ratra, B. The Cosmological Constant and Dark Energy. *Rev. Mod. Phys.* **75**, 559–606, DOI: [10.1103/RevModPhys.75.559](https://doi.org/10.1103/RevModPhys.75.559) (2003). [astro-ph/0207347](https://arxiv.org/abs/astro-ph/0207347).
175. Copeland, E. J., Sami, M. & Tsujikawa, S. Dynamics of dark energy. *Int. J. Mod. Phys. D15*, 1753–1936, DOI: [10.1142/S021827180600942X](https://doi.org/10.1142/S021827180600942X) (2006). [hep-th/0603057](https://arxiv.org/abs/hep-th/0603057).
176. Straumann, N. Dark energy. *Lect. Notes Phys.* **721**, 327–397, DOI: [10.1007/978-3-540-71117-9_13](https://doi.org/10.1007/978-3-540-71117-9_13) (2007).
177. Bass, S. D. The cosmological constant puzzle. *J. Phys. G38*, 043201, DOI: [10.1088/0954-3899/38/4/043201](https://doi.org/10.1088/0954-3899/38/4/043201) (2011).
178. Martin, J. Everything You Always Wanted To Know About The Cosmological Constant Problem (But Were Afraid To Ask). *Comptes Rendus Physique* **13**, 566–665, DOI: [10.1016/j.crhy.2012.04.008](https://doi.org/10.1016/j.crhy.2012.04.008) (2012). [1205.3365](https://arxiv.org/abs/1205.3365).
179. Dvali, G. & Gomez, C. Quantum Exclusion of Positive Cosmological Constant? *Annalen Phys.* **528**, 68–73, DOI: [10.1002/andp.201500216](https://doi.org/10.1002/andp.201500216) (2016). [1412.8077](https://arxiv.org/abs/1412.8077).
180. Laureijs, R. *et al.* Euclid definition study report (2011). [1110.3193](https://arxiv.org/abs/1110.3193).
181. Altarelli, G. Neutrino 2004: Concluding talk. *Nucl. Phys. Proc. Suppl.* **143**, 470–478, DOI: [10.1016/j.nuclphysbps.2005.01.146](https://doi.org/10.1016/j.nuclphysbps.2005.01.146) (2005). [hep-ph/0410101](https://arxiv.org/abs/hep-ph/0410101).
182. Bass, S. D. & Krzysiak, J. Vacuum energy with mass generation and Higgs bosons. *Phys. Lett. B* **803**, 135351, DOI: [10.1016/j.physletb.2020.135351](https://doi.org/10.1016/j.physletb.2020.135351) (2020). [2001.01706](https://arxiv.org/abs/2001.01706).
183. Trodden, M. Electroweak baryogenesis. *Rev. Mod. Phys.* **71**, 1463–1500, DOI: [10.1103/RevModPhys.71.1463](https://doi.org/10.1103/RevModPhys.71.1463) (1999). [hep-ph/9803479](https://arxiv.org/abs/hep-ph/9803479).
184. Morrissey, D. E. & Ramsey-Musolf, M. J. Electroweak baryogenesis. *New J. Phys.* **14**, 125003, DOI: [10.1088/1367-2630/14/12/125003](https://doi.org/10.1088/1367-2630/14/12/125003) (2012). [1206.2942](https://arxiv.org/abs/1206.2942).
185. Servant, G. The serendipity of electroweak baryogenesis. *Phil. Trans. Roy. Soc. Lond.* **A376**, 20170124, DOI: [10.1098/rsta.2017.0124](https://doi.org/10.1098/rsta.2017.0124) (2018). [1807.11507](https://arxiv.org/abs/1807.11507).
186. Amaro-Seoane, P. *et al.* Laser Interferometer Space Antenna. (2017). [1702.00786](https://arxiv.org/abs/1702.00786).
187. Caprini, C. *et al.* Science with the space-based interferometer eLISA. II: Gravitational waves from cosmological phase transitions. *JCAP* **1604**, 001, DOI: [10.1088/1475-7516/2016/04/001](https://doi.org/10.1088/1475-7516/2016/04/001) (2016). [1512.06239](https://arxiv.org/abs/1512.06239).
188. El-Neaj, Y. A. *et al.* AEDGE: Atomic Experiment for Dark Matter and Gravity Exploration in Space. *EPJ Quant. Technol.* **7**, 6, DOI: [10.1140/epjqt/s40507-020-0080-0](https://doi.org/10.1140/epjqt/s40507-020-0080-0) (2020). [1908.00802](https://arxiv.org/abs/1908.00802).
189. Bezrukov, F. L. & Shaposhnikov, M. The Standard Model Higgs boson as the inflaton. *Phys. Lett.* **B659**, 703–706, DOI: [10.1016/j.physletb.2007.11.072](https://doi.org/10.1016/j.physletb.2007.11.072) (2008). [0710.3755](https://arxiv.org/abs/0710.3755).
190. Jegerlehner, F. Higgs inflation and the cosmological constant. *Acta Phys. Polon.* **B45**, 1215, DOI: [10.5506/APhysPolB.45.1215](https://doi.org/10.5506/APhysPolB.45.1215) (2014). [1402.3738](https://arxiv.org/abs/1402.3738).
191. Rubio, J. Higgs inflation. *Front. Astron. Space Sci.* **5**, 50, DOI: [10.3389/fspas.2018.00050](https://doi.org/10.3389/fspas.2018.00050) (2019). [1807.02376](https://arxiv.org/abs/1807.02376).
192. Wetterich, C. Cosmology and the Fate of Dilatation Symmetry. *Nucl. Phys.* **B302**, 668–696, DOI: [10.1016/0550-3213\(88\)90193-9](https://doi.org/10.1016/0550-3213(88)90193-9) (1988). [1711.03844](https://arxiv.org/abs/1711.03844).
193. Peebles, P. J. E. & Ratra, B. Cosmology with a Time Variable Cosmological Constant. *Astrophys. J. Lett.* **325**, L17, DOI: [10.1086/185100](https://doi.org/10.1086/185100) (1988).

194. Capozziello, S. & De Laurentis, M. Extended Theories of Gravity. *Phys. Rept.* **509**, 167–321, DOI: [10.1016/j.physrep.2011.09.003](https://doi.org/10.1016/j.physrep.2011.09.003) (2011). [1108.6266](https://arxiv.org/abs/1108.6266).
195. Brüning, O. & Rossi, L. The High-Luminosity Large Hadron Collider. *Nat. Rev. Phys.* **1**, 241–243, DOI: [10.1038/s42254-019-0050-6](https://doi.org/10.1038/s42254-019-0050-6) (2019).
196. Abada, A. *et al.* FCC Physics Opportunities. *Eur. Phys. J.* **C79**, 474, DOI: [10.1140/epjc/s10052-019-6904-3](https://doi.org/10.1140/epjc/s10052-019-6904-3) (2019).
197. Gianotti, F. & Giudice, G. A roadmap for the future. *Nat. Phys.* **16**, 997–998, DOI: [10.1038/s41567-020-01054-6](https://doi.org/10.1038/s41567-020-01054-6) (2020).
198. *2020 Update of the European Strategy for Particle Physics* (CERN Council, Geneva, 2020).
199. Benedikt, M. & Zimmermann, F. The physics and technology of the Future Circular Collider. *Nat. Rev. Phys.* **1**, 238–240, DOI: [10.1038/s42254-019-0048-0](https://doi.org/10.1038/s42254-019-0048-0) (2019).
200. Benedikt, M., Blondel, A., Janot, P., Mangano, M. & Zimmermann, F. Future Circular Colliders succeeding the LHC. *Nat. Phys.* **16**, 402–407, DOI: [10.1038/s41567-020-0856-2](https://doi.org/10.1038/s41567-020-0856-2) (2020).
201. Stapnes, S. The Compact Linear Collider. *Nat. Rev. Phys.* **1**, 235–237, DOI: [10.1038/s42254-019-0051-5](https://doi.org/10.1038/s42254-019-0051-5) (2019).
202. Sicking, E. & Ström, R. From precision physics to the energy frontier with the Compact Linear Collider. *Nat. Phys.* **16**, 386–392, DOI: [10.1038/s41567-020-0834-8](https://doi.org/10.1038/s41567-020-0834-8) (2020). [2001.05224](https://arxiv.org/abs/2001.05224).
203. Michizono, S. The International Linear Collider. *Nat. Rev. Phys.* **1**, 244–245, DOI: [10.1038/s42254-019-0044-4](https://doi.org/10.1038/s42254-019-0044-4) (2019).
204. Lou, X. The Circular Electron Positron Collider. *Nat. Rev. Phys.* **1**, 232–234, DOI: [10.1038/s42254-019-0047-1](https://doi.org/10.1038/s42254-019-0047-1) (2019).
205. Agostini, M., Benato, G. & Detwiler, J. Discovery probability of next-generation neutrinoless double- β decay experiments. *Phys. Rev. D* **96**, 053001, DOI: [10.1103/PhysRevD.96.053001](https://doi.org/10.1103/PhysRevD.96.053001) (2017). [1705.02996](https://arxiv.org/abs/1705.02996).
206. Caldwell, A., Merle, A., Schulz, O. & Totzauer, M. Global Bayesian analysis of neutrino mass data. *Phys. Rev. D* **96**, 073001, DOI: [10.1103/PhysRevD.96.073001](https://doi.org/10.1103/PhysRevD.96.073001) (2017). [1705.01945](https://arxiv.org/abs/1705.01945).

Acknowledgements

None of the results presented in this review would have been possible without the diligent efforts of all our colleagues from the LHC accelerator group, the ATLAS and CMS experiments, the computing divisions, the theoretical community and many more, whom all took part in this fantastic adventure at the energy frontier. Specifically we like to thank Maria Cepeda, Fred Jegerlehner and Janina Krzysiak for sharing their insight and useful discussions in the preparation of this manuscript.